

Appendix A

Analysis of the arc signals acquired during wet welding

	Page
A.1 Arc voltage signals	A.1
A.2 Arc voltage signals with direct current electrode positive (DCEP)	A.3
A.2.1 BOP welds on A36 Steel	A.4
A.2.2 BOP welds on A572 Gr. 50 Steel	A.8
A.2.3 BOP welds on API 5L Gr. B steel	A.12
A.3 Arc voltage signals with direct current electrode negative (DCEN)	A.17
A.3.1 BOP welds on A36 steel	A.18
A.3.2 BOP welds on A572 Gr. 50 steel	A.22
A.3.3 BOP welds on API 5L Gr. B steel	A.26
A.4 Arc current signals with direct current electrode positive (DCEP)	A.30
A.4.1 BOP welds on A36 steel	A.31
A.4.2 BOP welds on A572 Gr. 50 steel	A.33
A.4.3 BOP welds on API 5L Gr. B steel	A.35
A.5 Arc current signals with direct current electrode negative (DCEN)	A.37
A.5.1 BOP welds on A36 steel	A.38
A.5.2 BOP welds on A572 Gr. 50 steel	A.40
A.5.3 BOP welds on API 5L Gr. B steel	A.42
A.6 Summary of results	A.44

List of Tables

Table A.1 Metal transfer modes in the shielded metal arc welding (SMAW) process. .	A.2
Table A.2. Summary of welding parameter from the bead-on-plate wet welds deposited with three electrodes on three steel types and at two water depths.	A.44
Table A.3. Metal transfer modes observed in wet welds deposited with three electrode types on three steels at two water depths.	A.45

List of Figures

Figure A.1. Illustration of the arc length during welding with covered electrodes (a) arc length without droplet, and (b) arc length with droplet.	A.1
Figure A.2. Voltage signals recorded during wet welding with (a) E6013, (b) E7018, and (c) E7024 electrode type on A36 steel at 50 m water depth.	A.4
Figure A.3. Power spectral density of the voltage signals acquired during wet welding at 50 m with (a) E6013, (b) E7018, and (c) E7024 electrode type.	A.5
Figure A.4. Voltage signals recorded during wet welding with (a) E6013, (b) E7018, and (c) E7024 electrode type on A36 steel at 100 m water depth.	A.6
Figure A.5. Power spectral density of the voltage signals acquired during wet welding at 100 m with (a) E6013, (b) E7018, and (c) E7024 electrode type.	A.7

Figure A.6. Voltage signals recorded during wet welding with (a) E6013, (b) E7018, and (c) E7024 electrode type on A572 Gr. 50 steel at 50 m water depth. A.8

Figure A.7. Spectra of the voltage signals acquired during wet welding at 50 m with (a) E6013, (b) E7018, and (c) E7024 electrode type on A572 Gr. 50 steel. A.9

Figure A.8. Voltage signals recorded during wet welding with (a) E6013, (b) E7018, and (c) E7024 electrode type on A572 Gr. 50 steel at 100 m water depth. A.10

Figure A.9. Spectra of the voltage signals acquired during wet welding at 100 m with (a) E6013, (b) E7018, and (c) E7024 electrode on A572 Gr. 50 steel. A.11

Figure A.10. Voltage signals recorded during wet welding with (a) E6013, (b) E7018, and (c) E7024 electrode type on API 5L Gr. B steel at 50 m water depth. A.13

Figure A.11. Spectra of the voltage signals acquired during wet welding at 50 m with (a) E6013, (b) E7018, and (c) E7024 electrode type on API 5L Gr. B steel. A.14

Figure A.12. Voltage signals recorded during wet welding with (a) E6013, (b) E7018, and (c) E7024 electrode type on API 5L Gr. B steel at 100 m water depth. A.15

Figure A.13. Spectra of the voltage signals acquired during wet welding at 100 m with (a) E6013, (b) E7018, and (c) E7024 electrode type on API 5L Gr. B steel. A.16

Figure A.14. Voltage signals recorded during wet welding with (a) E6013, (b) E7018, and (c) E7024 electrode type on A36 steel at 50 m water depth. A.18

Figure A.15. Power spectral density of the voltage signals acquired during wet welding at 50 m with (a) E6013, (b) E7018, and (c) E7024 electrode type. A.19

Figure A.16. Voltage signals recorded during wet welding with (a) E6013, (b) E7018, and (c) E7024 electrode type on A36 steel at 100 m water depth. A.20

Figure A.17. Power spectral density of the voltage signals acquired during wet welding at 100 m with (a) E6013, (b) E7018, and (c) E7024 electrode type. A.21

Figure A.18. Voltage signals recorded during wet welding with (a) E6013, (b) E7018, and (c) E7024 electrode type on A572 Gr. 50 steel at 50 m water depth. A.22

Figure A.19. Power spectral density of the voltage signals acquired during wet welding at 50 m with (a) E6013, (b) E7018, and (c) E7024 electrode type on A572 Gr. 50 steel. A.23

Figure A.20. Voltage signals recorded during wet welding with (a) E6013, (b) E7018, and (c) E7024 electrode type on A572 Gr. 50 steel at 100 m water depth. A.24

Figure A.21. Power spectral density of the voltage signals acquired during wet welding at 100 m with (a) E6013, (b) E7018, and (c) E7024 electrode type on A572 Gr. 50 steel. A.25

Figure A.22. Voltage signals recorded during wet welding with (a) E6013, (b) E7018, and (c) E7024 electrode type on API 5L Gr. B steel at 50 m water depth. A.26

Figure A.23. Power spectral density of the voltage signals acquired during wet welding at 50 m with (a) E6013, (b) E7018, and (c) E7024 electrode type on API 5L Gr. B steel. A.27

Figure A.24. Voltage signals recorded during wet welding with (a) E6013, (b) E7018, and (c) E7024 electrode type on API 5L Gr. B steel at 100 m water depth. A.28

Figure A.25. Power spectral density of the voltage signals acquired during wet welding at 100 m with (a) E6013, (b) E7018, and (c) E7024 electrode type on API 5L Gr. B steel. A.29

Figure A.26. Arc current signals from wet welds deposited with (a) E6013, (b) E7018, and (c) E7024 electrode type at 50 m. A.31

Figure A.27. Arc current signals from wet welds deposited with (a) E6013, (b) E7018, and (c) E7024 electrode type at 100 m. A.32

Figure A.28. Arc current signals from wet welds deposited with (a) E6013, (b) E7018, and (c) E7024 electrode type at 50 m. A.33

Figure A.29. Arc current signals from wet welds deposited with (a) E6013, (b) E7018, and (c) E7024 electrode type at 100 m. A.34

Figure A.30. Arc current signals from wet welds deposited with (a) E6013, (b) E7018, and (c) E7024 electrode type at 50 m. A.35

Figure A.31. Arc current signals from wet welds deposited with (a) E6013, (b) E7018, and (c) E7024 electrode type at 100 m. A.36

Figure A.32. Arc current signals from wet welds deposited with (a) E6013, (b) E7018, and (c) E7024 electrode type at 50 m. A.38

Figure A.33. Arc current signals from wet welds deposited with (a) E6013, (b) E7018, and (c) E7024 electrode type at 100 m. A.39

Figure A.34. Arc current signals from wet welds deposited with (a) E6013, (b) E7018, and (c) E7024 electrode type at 50 m. A.40

Figure A.35. Arc current signals from wet welds deposited with (a) E6013, (b) E7018, and (c) E7024 electrode type at 100 m. A.41

Figure A.36. Arc current signals from wet welds deposited with (a) E6013, (b) E7018, and (c) E7024 electrode type at 50 m. A.42

Figure A.37. Arc current signals from wet welds deposited with (a) E6013, (b) E7018, and (c) E7024 electrode type at 100 m. A.43

A.1 Arc voltage signals

Bead-on-plate (BOP) wet welds were deposited with three electrodes (E6013, E7018 and E7024) on the three steels (A36, A572 Gr. 50, and API 5L Gr. B) at two water depths (50 and 100 m). Shielded metal arc welding (SMAW) process with direct current electrode positive (DCEP) and direct current electrode negative (DCEN) polarities were used.

When the arc starts liquid metal droplets form at the electrode tip and after reaching certain size transfer to the weld pool. At the same time the flux covering melts forming a truncated cone at the electrode tip as shown in Figure 1 (a) and (b). From Figure 1 (a) one could say that the arc length, which is the distance between the tip of the electrode rod to the liquid metal in the weld pool depends on the flux covering thickness of the electrode (the thicker the flux covering the larger the arc length). With the gravity welding system used in the research program, as soon as the arc starts the electrode drags on the plate surface during welding. The external side of the electrode flux covering is in contact with the plate surface. In Figure 1 (a) and (b) the distances between the electrode tip and the weld pool, as well as the distance from the droplet to the weld pool are given by the arc voltage signal. As the droplet grows the distance d between the droplet and the weld pool decreases. Similarly, as d decreases the arc voltage decreases. Thereafter, arc voltage fluctuations are associated with the fluctuations in droplet size and breakage of the flux wall could be responsible for voltage drops during welding.

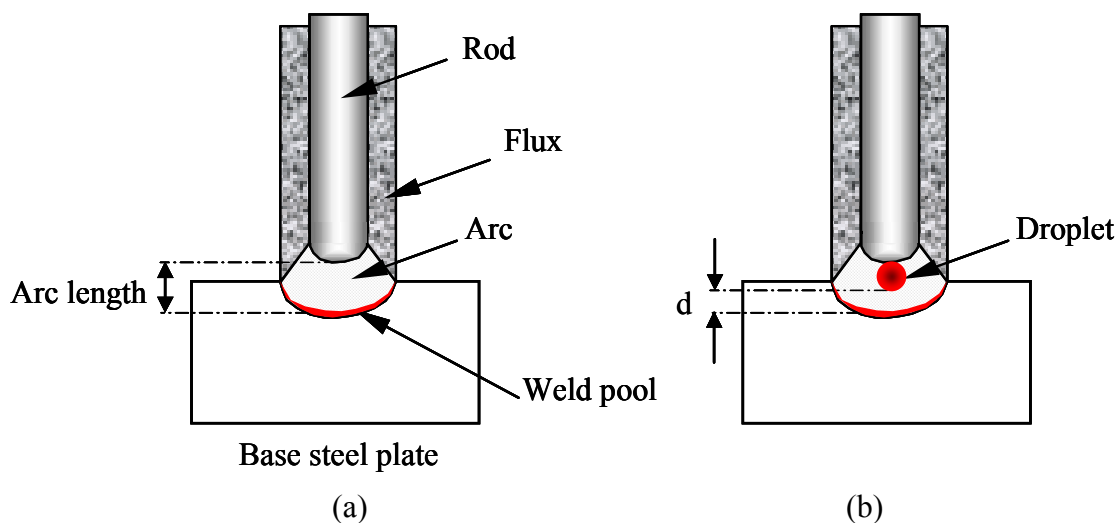


Figure A.1. Illustration of the arc length during welding with covered electrodes (a) arc length without droplet, and (b) arc length with droplet.

The way in which liquid metal passes from the electrode tip to the plate is known as metal transfer mode, which according to the nomenclature used by the International Institute of Welding (IIW), can be classified as follows:

1. Free-flight transfer (globular, spray and explosive)
2. Bridging transfer (short-circuiting and bridging without interruption)
3. Slag protected transfer (flux-wall guided)

In the shielded metal arc welding (SMAW) process globular/explosive, short-circuiting and slag-protected are the commonly observed metal transfer modes. In order to know the metal transfer modes of the commercial electrodes used in this work, arc signals were recorded for analysis. The arc signals were acquired at rate of 250 samples per second. The arc signals recording started just before starting the arc and ended immediately after the arc extinction. In this way the welding time was calculated from the recorded signals.

Metal transfer modes can be qualitatively and quantitatively determined from the arc voltage signals in the time domain and the corresponding spectra in the frequency domain as shown in table 1.

Table A.1 Metal transfer modes in the shielded metal arc welding (SMAW) process.

Metal transfer mode	Time domain	Frequency domain	Comments
Spray	Small fluctuations	Peaks at high frequencies	Not important in wet welds with SMAW process
Globular	Large voltage fluctuations	Peaks at low frequencies	Present in the SMAW process, Fig. 2(c)
Short-circuiting	Large voltage drops tending to zero volts	Peaks at low frequencies	Present in the SMAW process, Fig. 2(b)

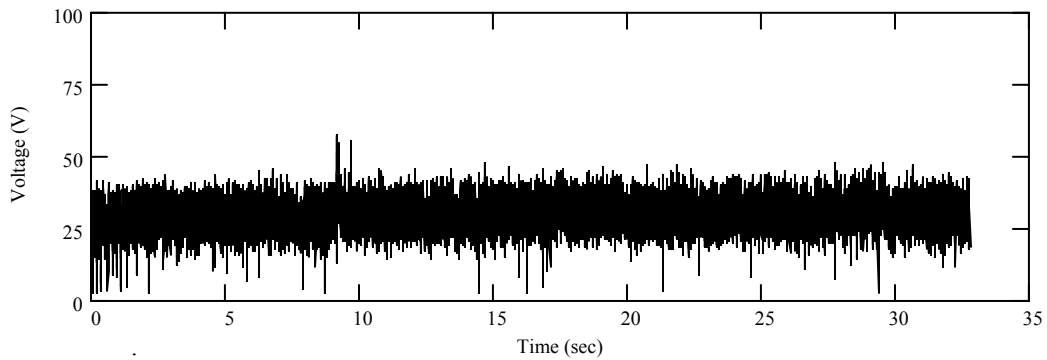
A.2 Arc voltage signals with direct current electrode positive (DCEP)

In order to know the metal transfer modes present during wet welding with the different electrodes, welding arc signals were recorded. Figures A.2, A.4, A.6, A.8, A.10, and A.12 present the voltage signals acquired during welding with the three electrodes on the three steels at two water depths. Similarly, Figures A.3, A.5, A.7, A.9, A.11 and A.13 present the corresponding calculated spectra of the voltage signals before mentioned.

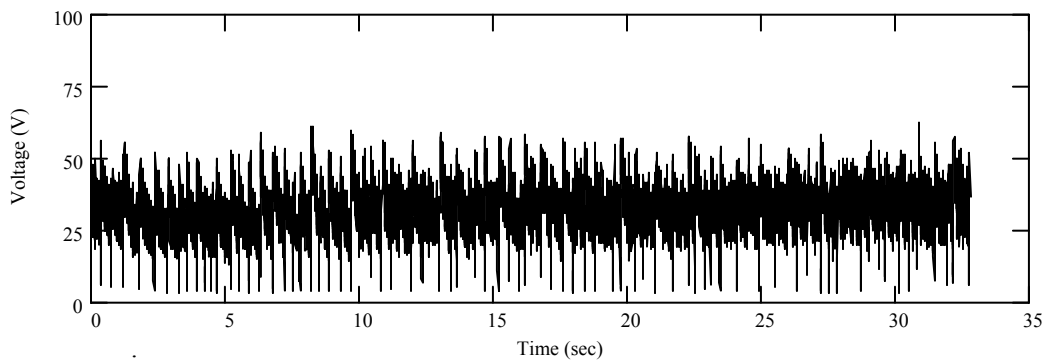
Power spectral densities of the voltage signals were calculated using Fast Fourier Transform (FFT) technique. To calculate the spectra 8192 data points were used in most of the analyzed cases, only a few of them were analyzed with 4096 data points.

A.2.1 BOP welds on A36 Steel

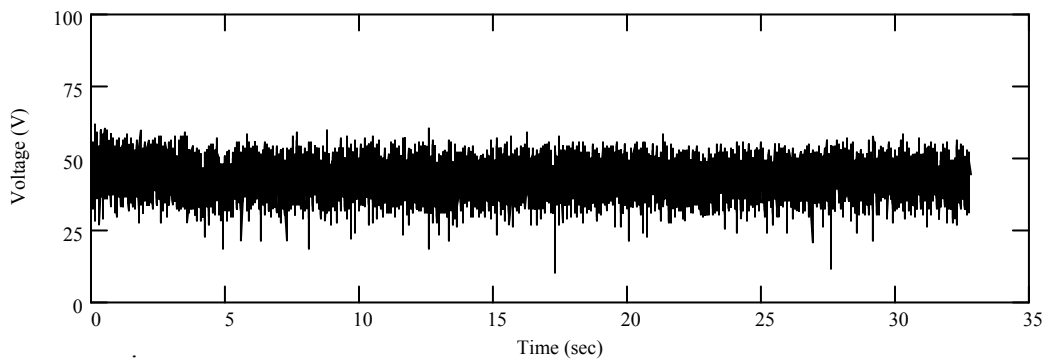
Figures A.2 and A.4 correspond to arc voltage signals in the time domain and its associated spectra are shown in Figure A.3 and A.5. The BOP wet welds were deposited with E6013, E7018, and E7024 electrode type on A36 steel at 50 and 100m.



(a) Globular with few short-circuiting indications

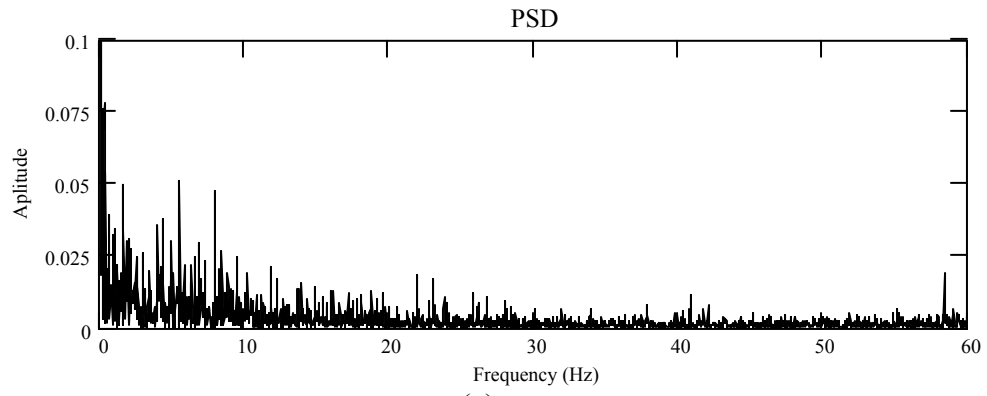


(b) Short-circuiting

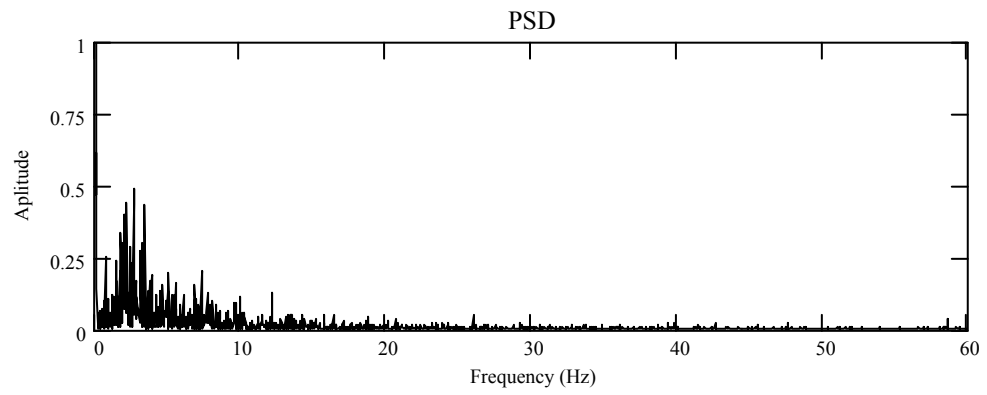


(c) Globular

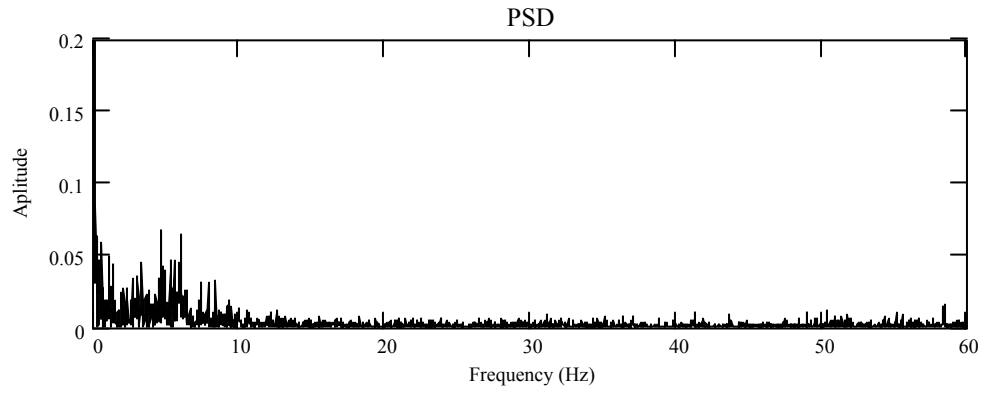
Figure A.2. Voltage signals recorded during wet welding with (a) E6013, (b) E7018, and (c) E7024 electrode type on A36 steel at 50 m water depth.



(a)

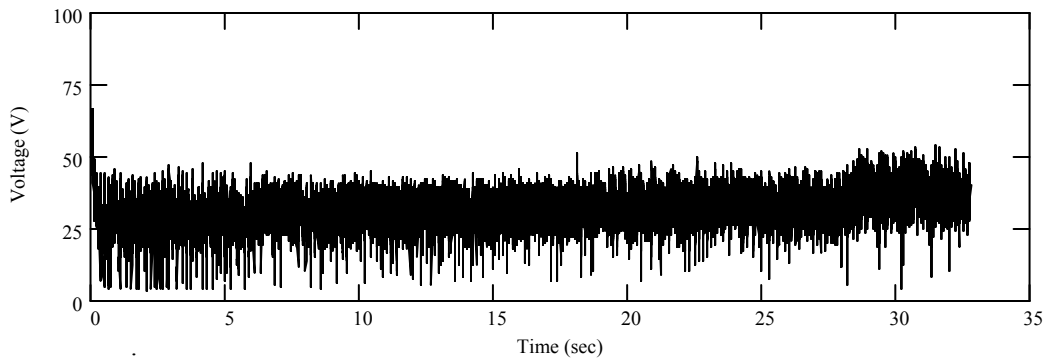


(b)

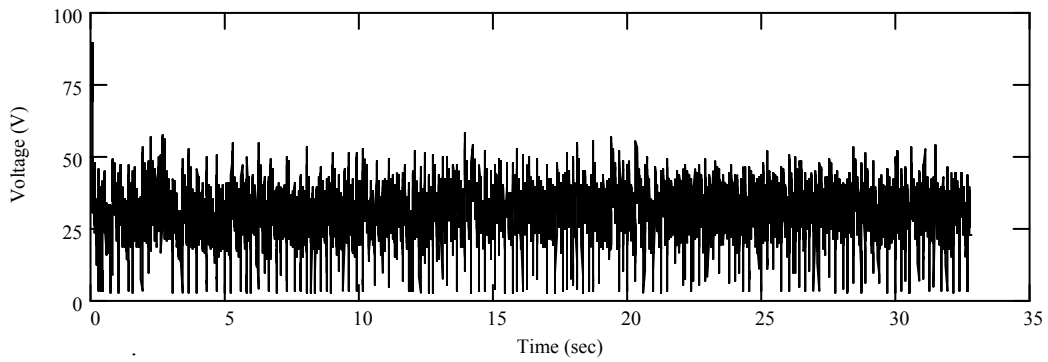


(c)

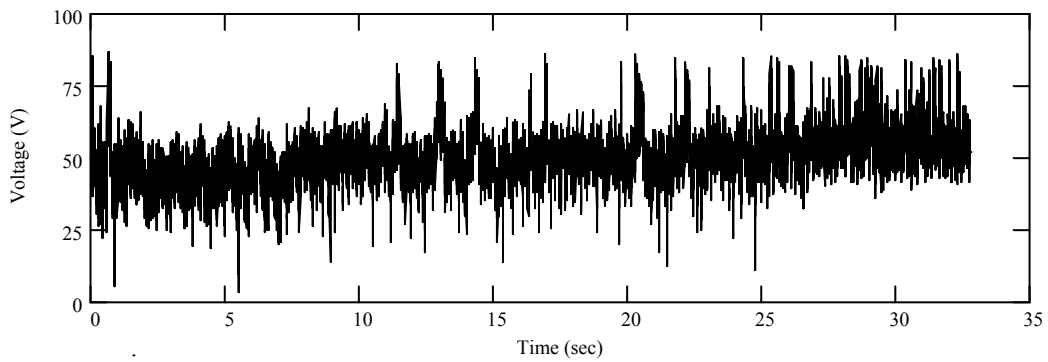
Figure A.3. Power spectral density of the voltage signals acquired during wet welding at 50 m with (a) E6013, (b) E7018, and (c) E7024 electrode type.



(a) Globular and short-circuiting

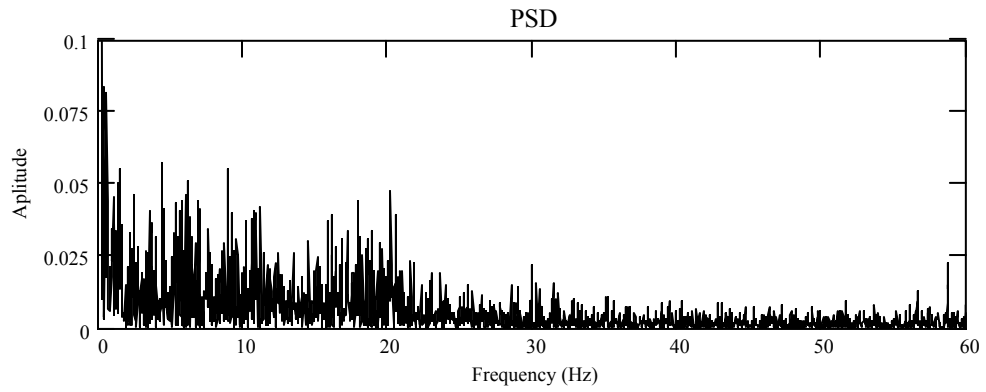


(b) Short-circuiting

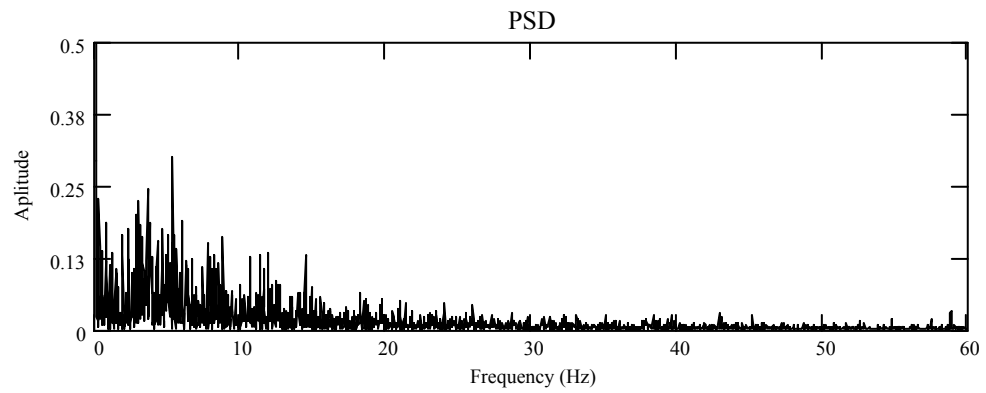


(c) Globular

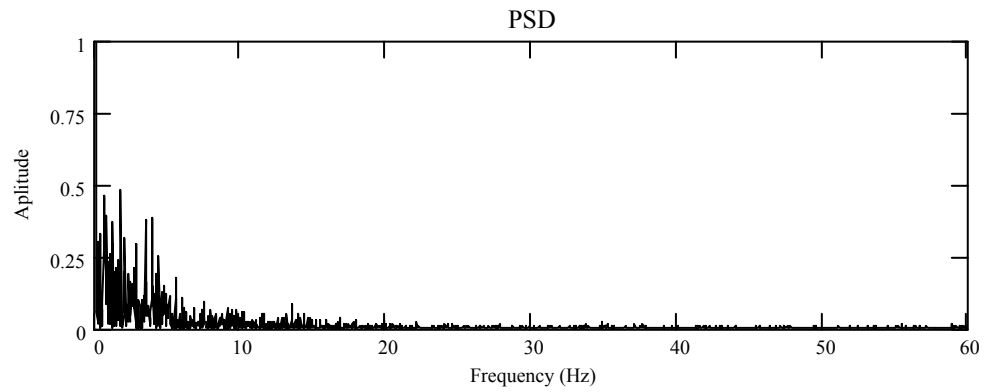
Figure A.4. Voltage signals recorded during wet welding with (a) E6013, (b) E7018, and (c) E7024 electrode type on A36 steel at 100 m water depth.



(a)



(b)

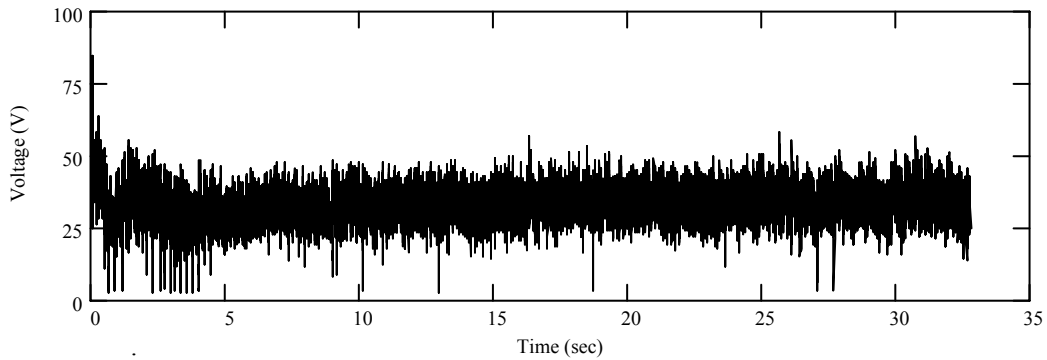


(c)

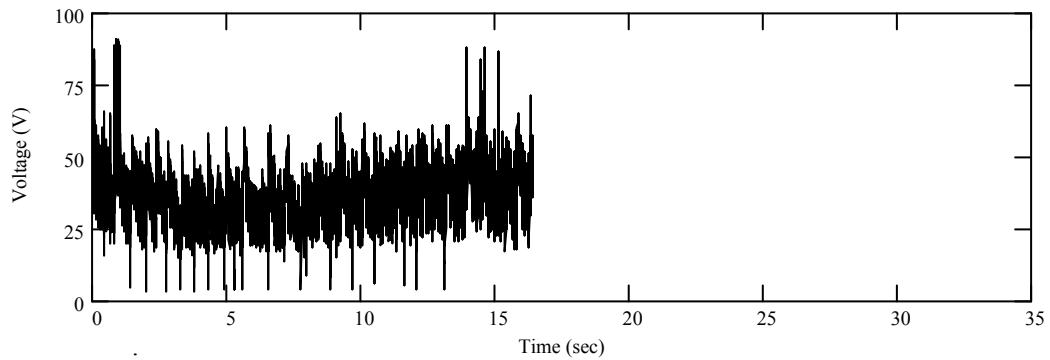
Figure A.5. Power spectral density of the voltage signals acquired during wet welding at 100 m with (a) E6013, (b) E7018, and (c) E7024 electrode type.

A.2.2 BOP welds on A572 Gr. 50 Steel

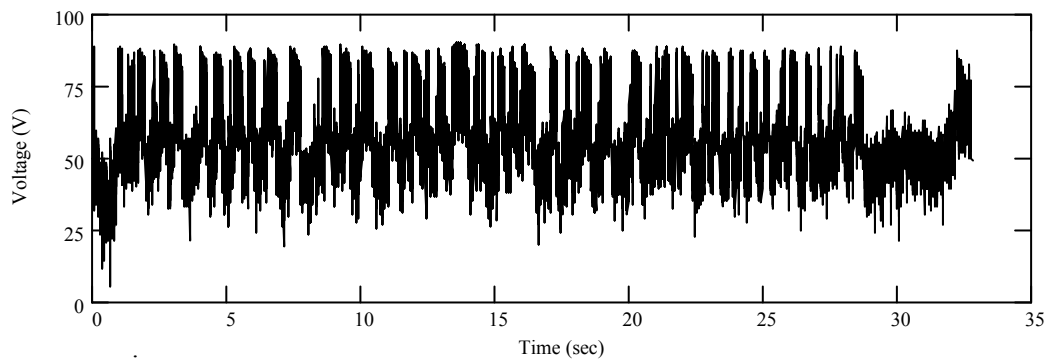
Figures A.6 and A.8 correspond to arc voltage signals in the time domain and its associated spectra are shown in Figure A.7 and A.9. The BOP wet welds were deposited with E6013, E7018, and E7024 electrode type on A572 Gr. 50 steel at 50 and 100m.



(a) Short-circuiting at the beginning then globular



(b) Short-circuiting and globular



(c) Globular

Figure A.6. Voltage signals recorded during wet welding with (a) E6013, (b) E7018, and (c) E7024 electrode type on A572 Gr. 50 steel at 50 m water depth.

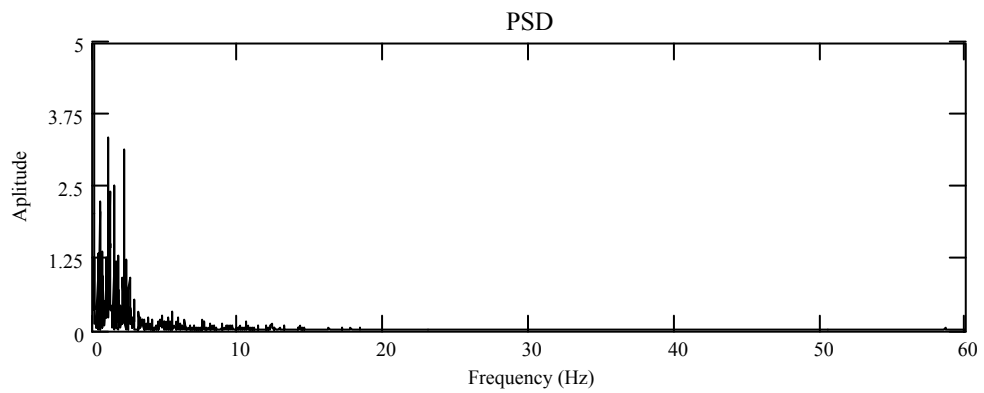
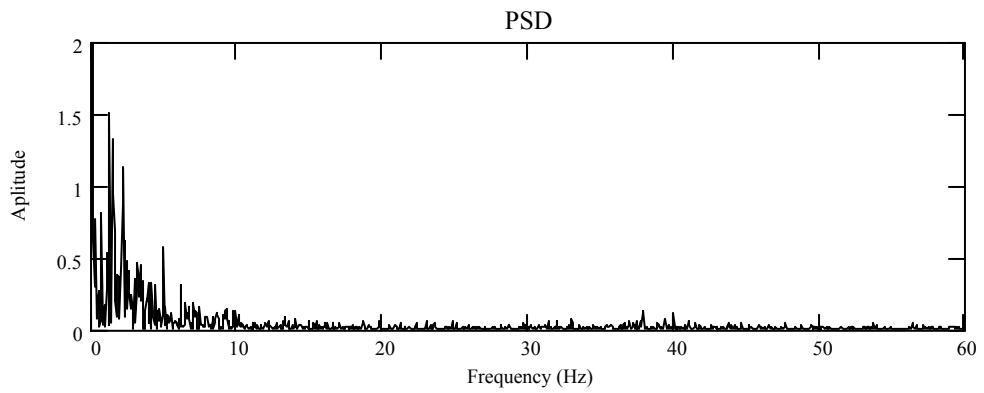
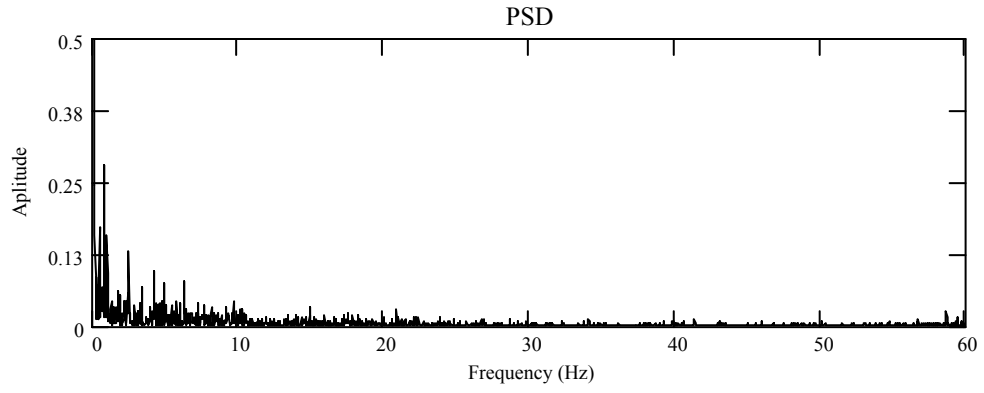
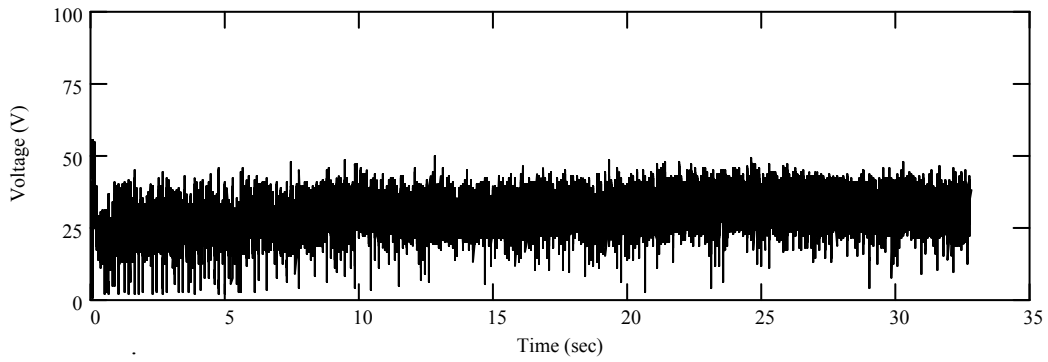
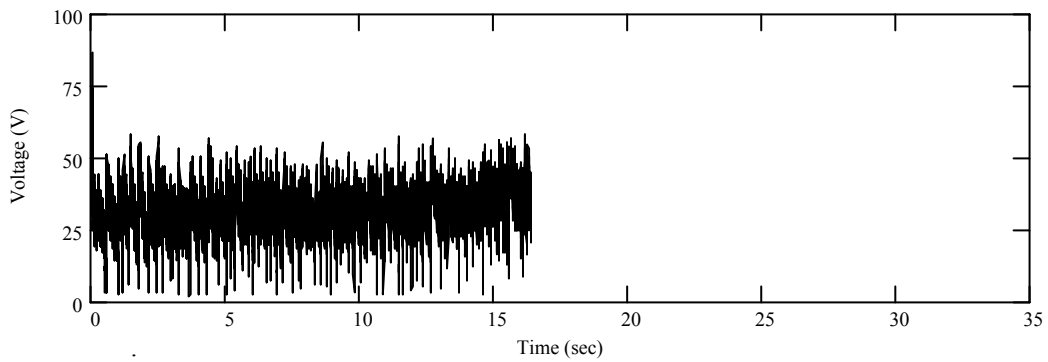


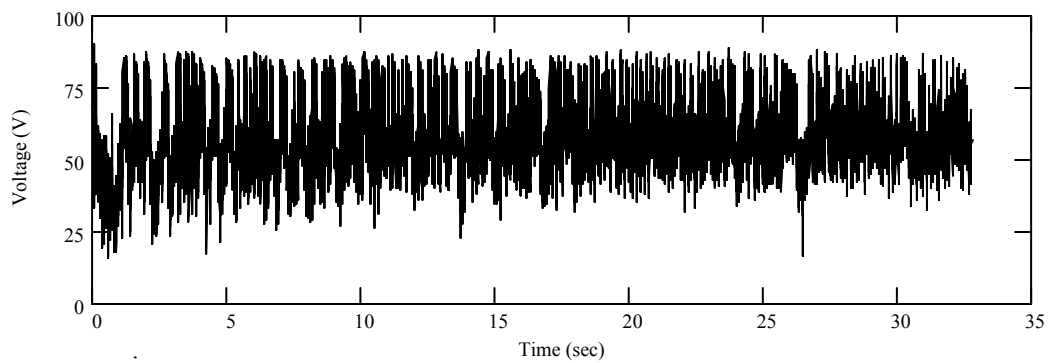
Figure A.7. Spectra of the voltage signals acquired during wet welding at 50 m with (a) E6013, (b) E7018, and (c) E7024 electrode type on A572 Gr. 50 steel.



(a) Short-circuiting in the first 12 sec. then globular



(b) Short-circuiting



(c) Globular

Figure A.8. Voltage signals recorded during wet welding with (a) E6013, (b) E7018, and (c) E7024 electrode type on A572 Gr. 50 steel at 100 m water depth.

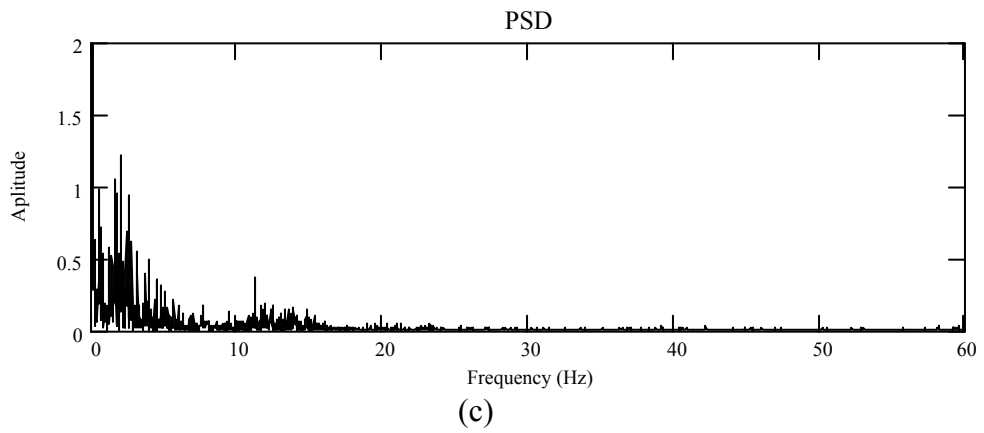
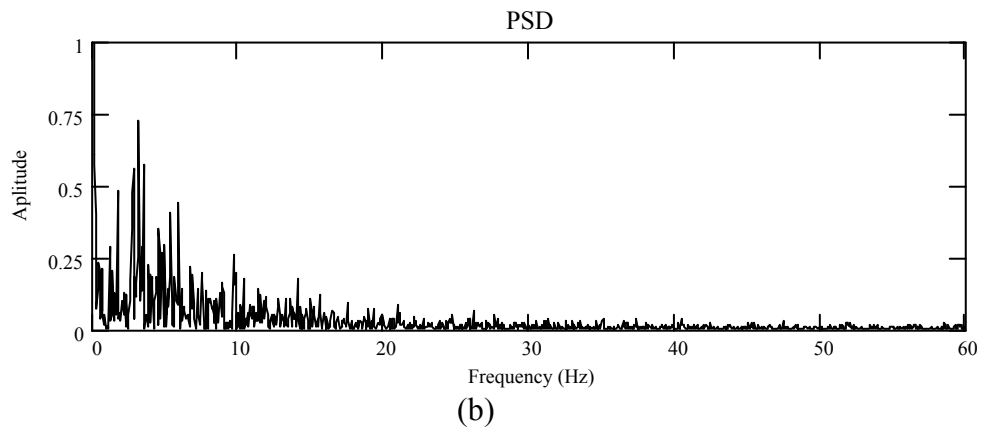
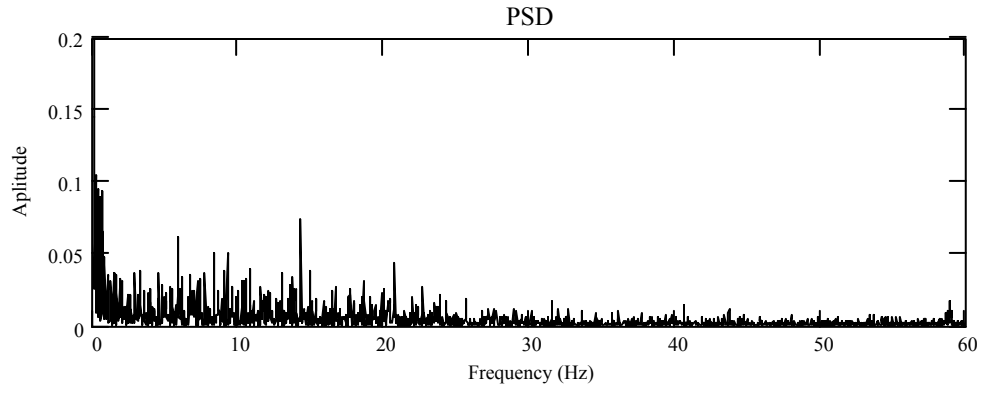
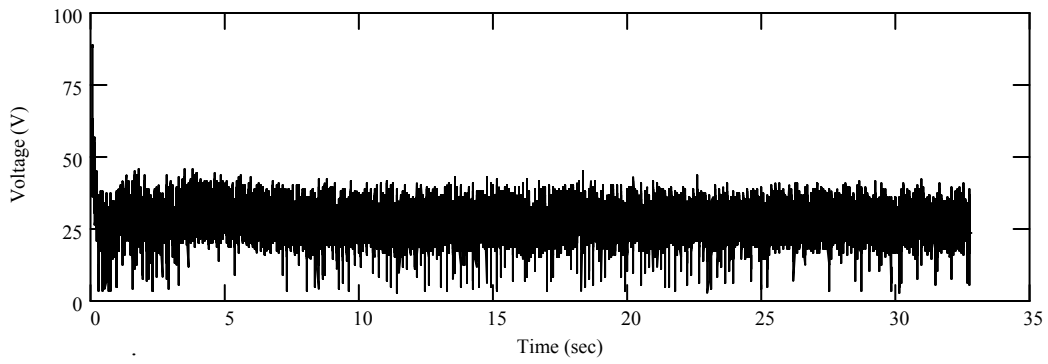


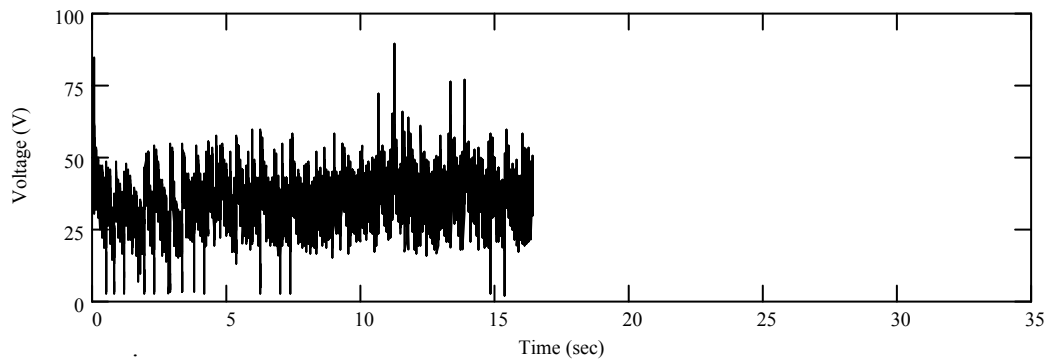
Figure A.9. Spectra of the voltage signals acquired during wet welding at 100 m with (a) E6013, (b) E7018, and (c) E7024 electrode on A572 Gr. 50 steel.

A.2.3 BOP welds on API 5L Gr. B steel

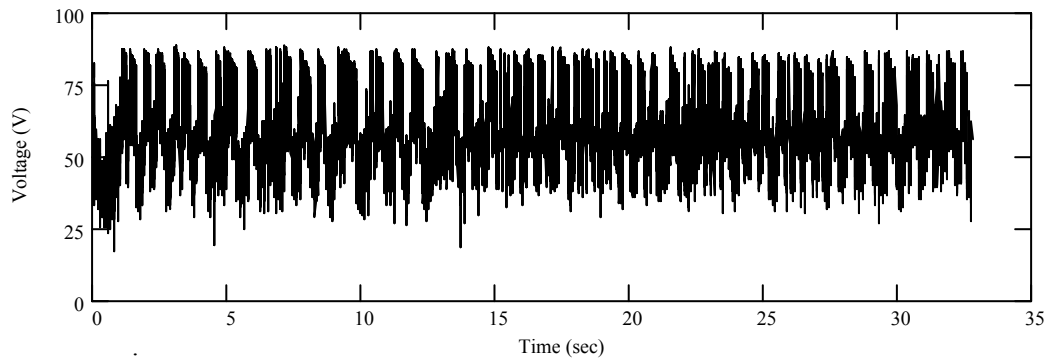
Figures A.10 and A.12 correspond to arc voltage signals in the time domain and its associated spectra are shown in Figure A.11 and A.13. The BOP wet welds were deposited with E6013, E7018, and E7024 electrode type on API 5L Gr. B steel at 50 and 100m.



(a) Short-circuiting and globular

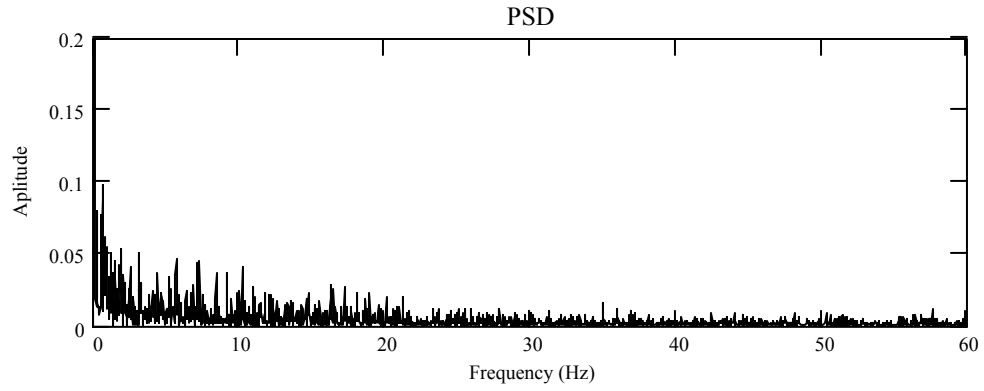


(b) Short-circuiting and globular

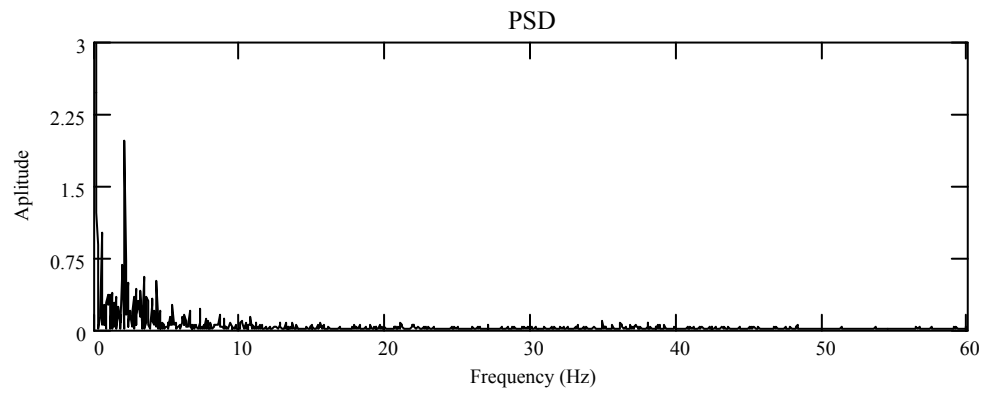


(c) Globular

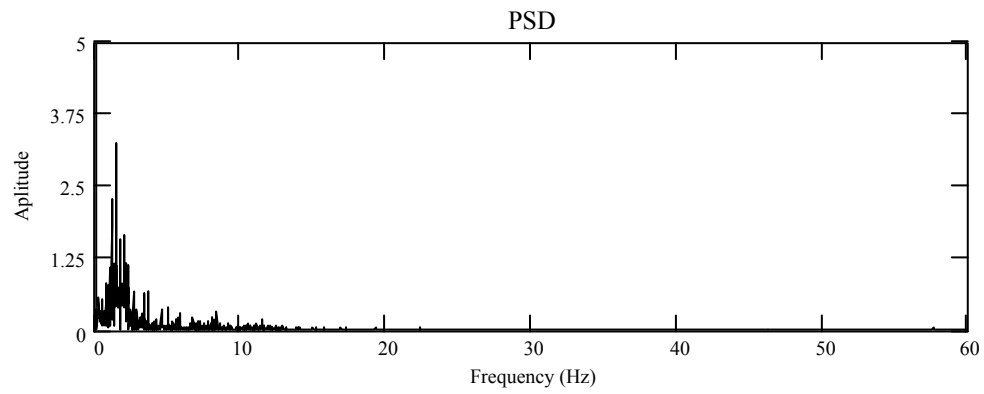
Figure A.10. Voltage signals recorded during wet welding with (a) E6013, (b) E7018, and (c) E7024 electrode type on API 5L Gr. B steel at 50 m water depth.



(a)

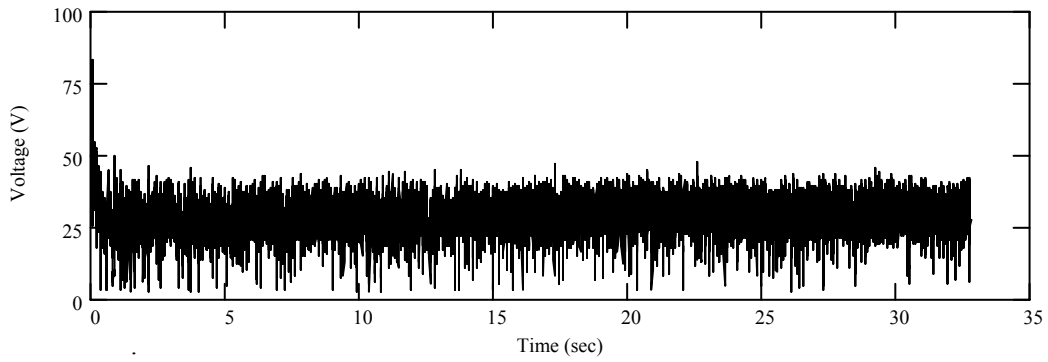


(b)

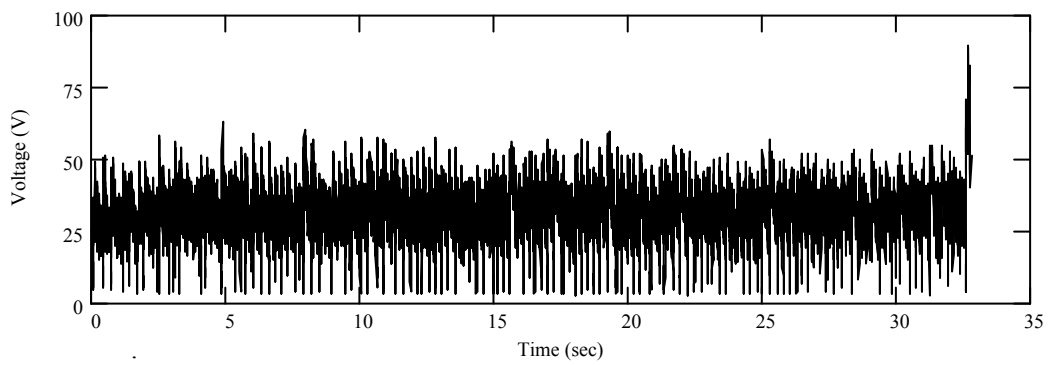


(c)

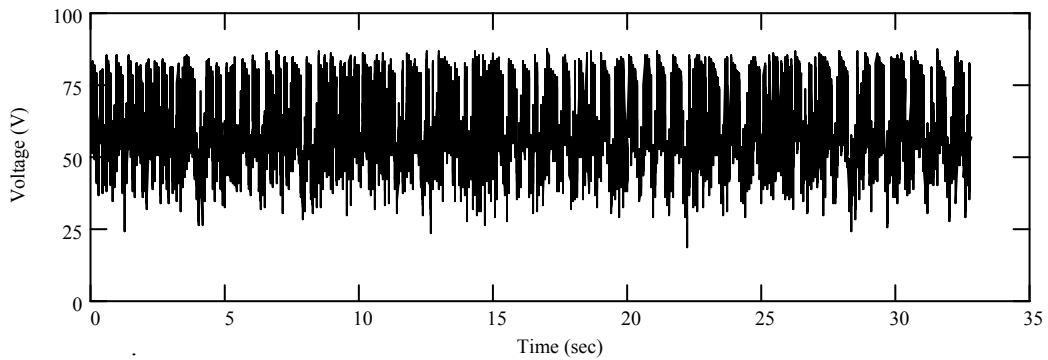
Figure A.11. Spectra of the voltage signals acquired during wet welding at 50 m with (a) E6013, (b) E7018, and (c) E7024 electrode type on API 5L Gr. B steel.



(a) Short-circuiting and globular



(b) Short-circuiting



(c) Globular

Figure A.12. Voltage signals recorded during wet welding with (a) E6013, (b) E7018, and (c) E7024 electrode type on API 5L Gr. B steel at 100 m water depth.

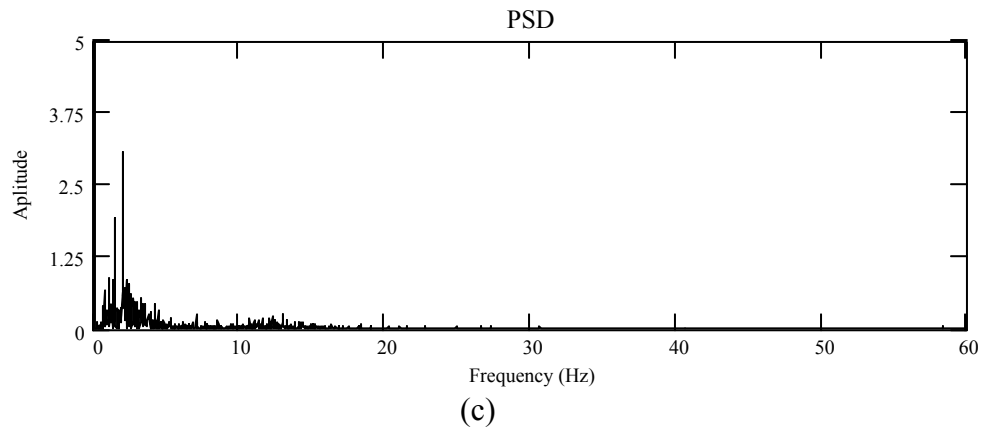
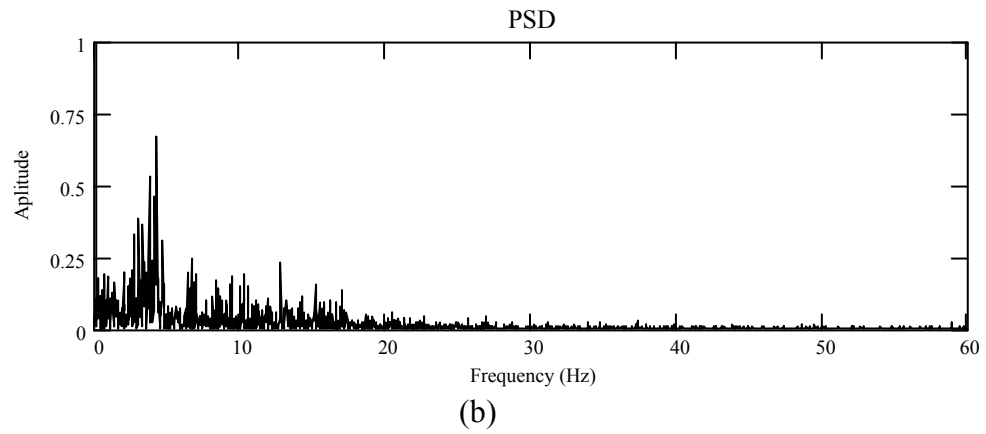
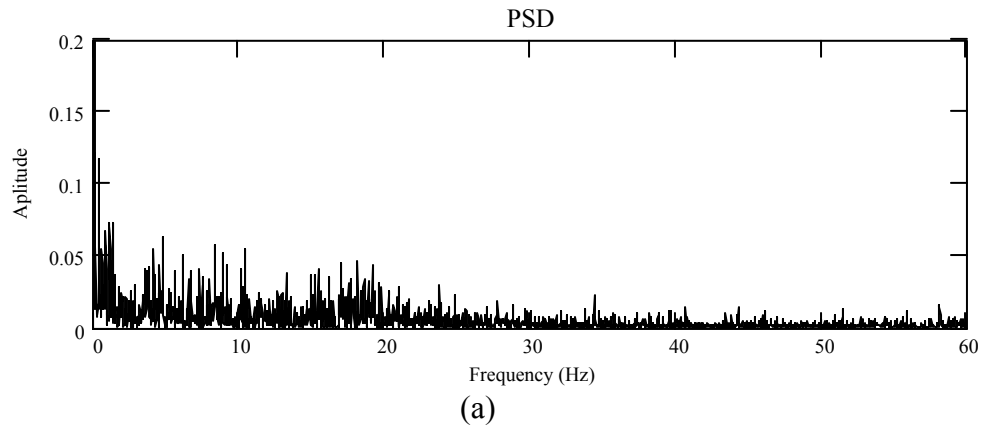


Figure A.13. Spectra of the voltage signals acquired during wet welding at 100 m with (a) E6013, (b) E7018, and (c) E7024 electrode type on API 5L Gr. B steel.

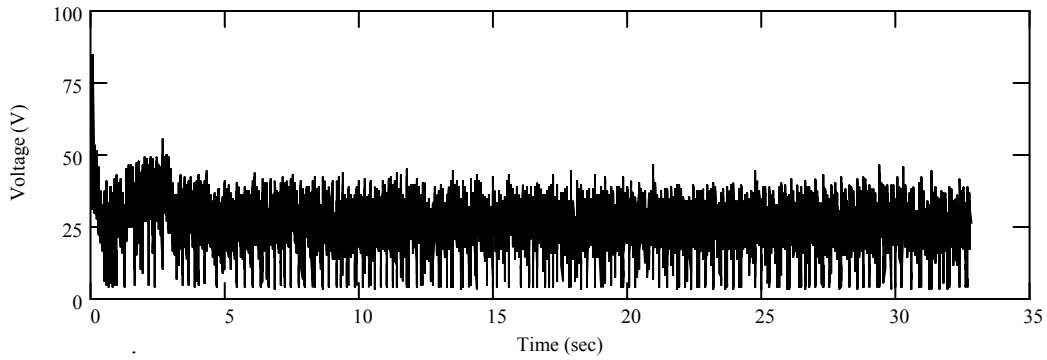
A.3 Arc voltage signals with direct current electrode negative (DCEN)

Figures A.14, A.16, A.18, A.20, A.22, and A.24 present the voltage signals acquired during welding with the three electrodes on the three steels at two water depths. Similarly, Figures A.15, A.17, A.19, A.21, A.23, and A.25 present the calculated spectra of the voltage signals before mentioned.

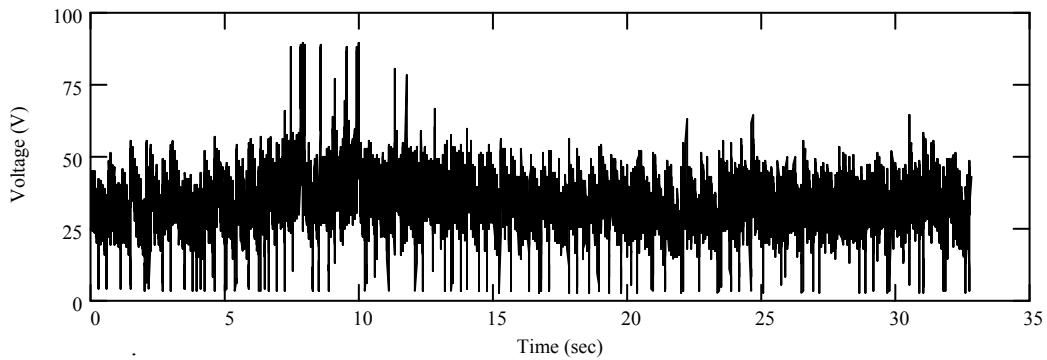
As above mentioned power spectral densities of the voltage signals were calculated using the FFT technique. To calculate the spectra 8192 data points were used in most of the cases, only a few of them were analyzed with 4096 data points.

A.3.1 BOP welds on A36 steel

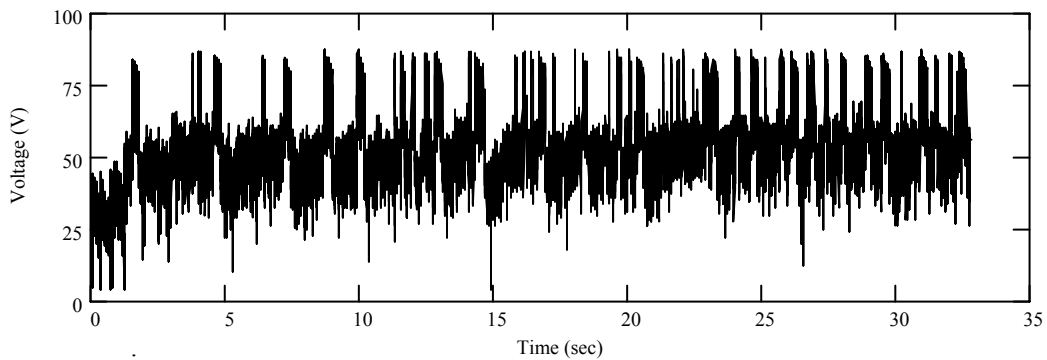
Figures A.14 and A.16 correspond to arc voltage signals in the time domain and its associated spectra are shown in Figure A.15 and A.17. The BOP wet welds were deposited with E6013, E7018, and E7024 electrode type on A36 steel at 50 and 100m.



(a) Short-circuiting



(b) Short-circuiting and globular



(c) Globular

Figure A.14. Voltage signals recorded during wet welding with (a) E6013, (b) E7018, and (c) E7024 electrode type on A36 steel at 50 m water depth.

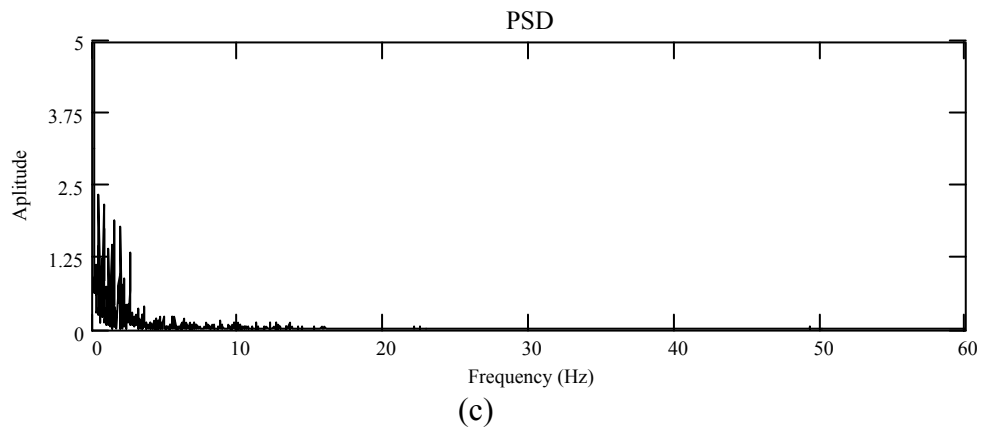
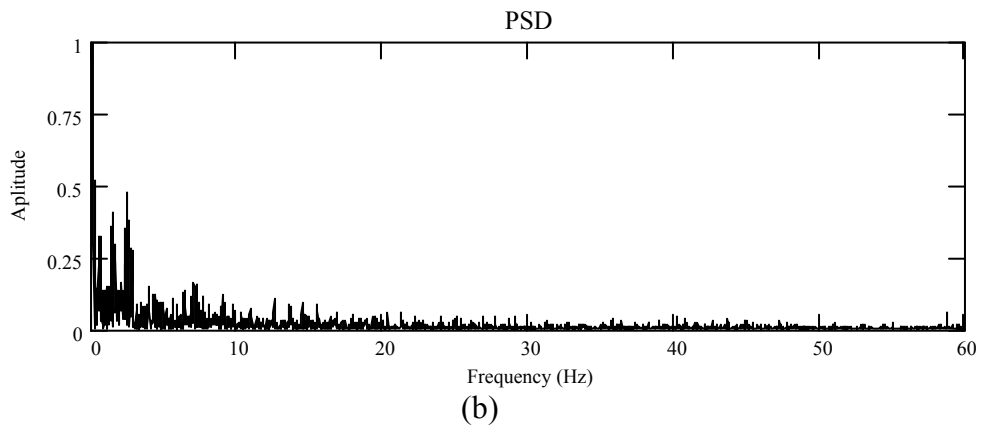
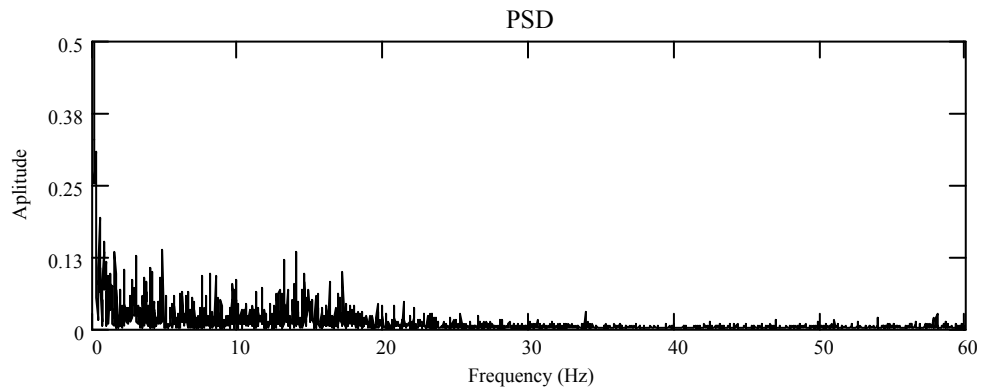
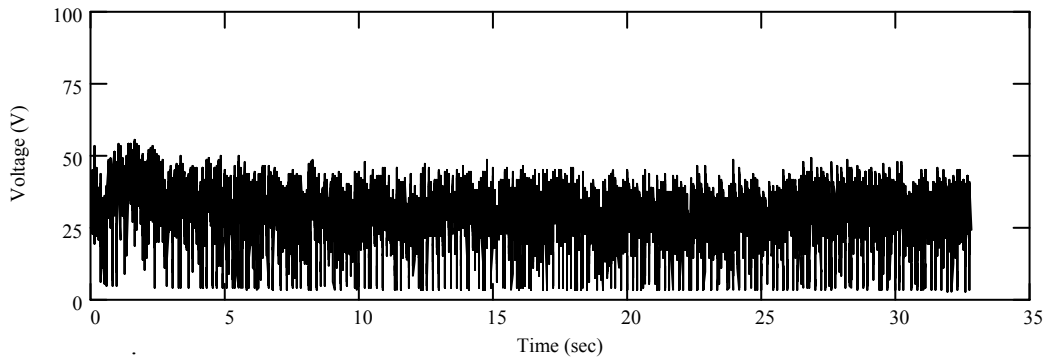
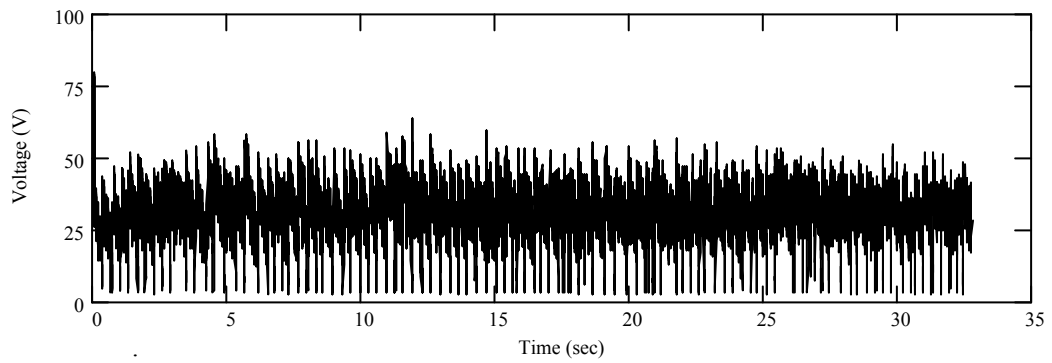


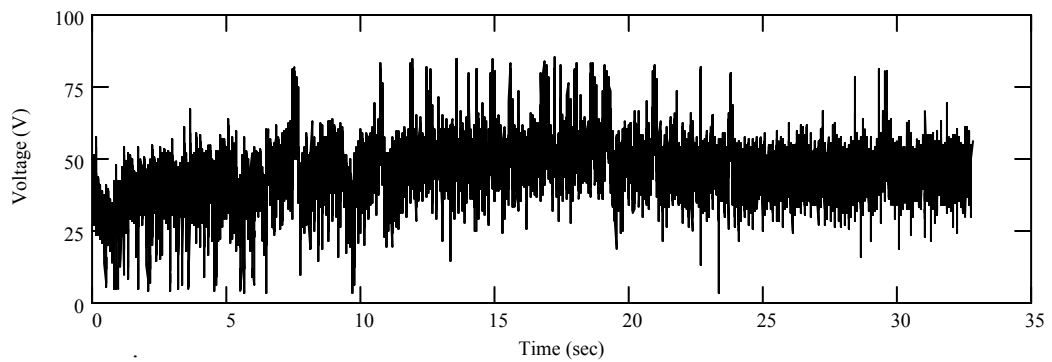
Figure A.15. Power spectral density of the voltage signals acquired during wet welding at 50 m with (a) E6013, (b) E7018, and (c) E7024 electrode type.



(a) Short-circuiting



(b) Short-circuiting



(c) Globular with few short-circuiting

Figure A.16. Voltage signals recorded during wet welding with (a) E6013, (b) E7018, and (c) E7024 electrode type on A36 steel at 100 m water depth.

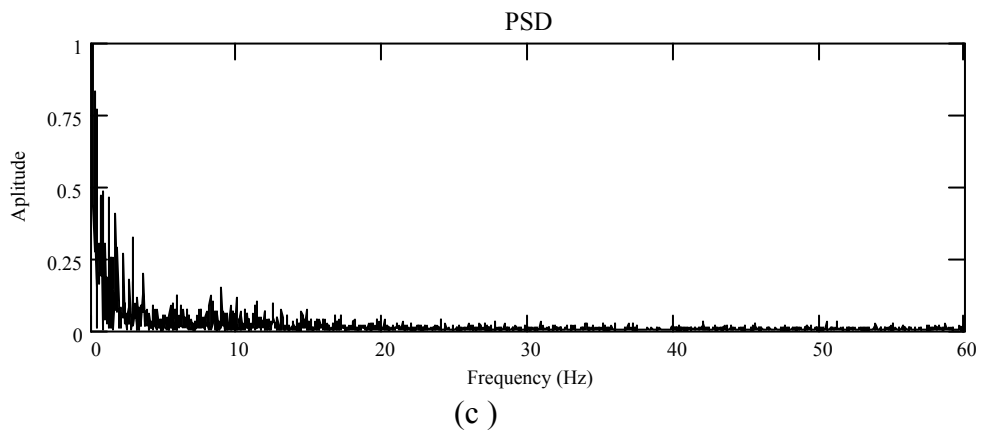
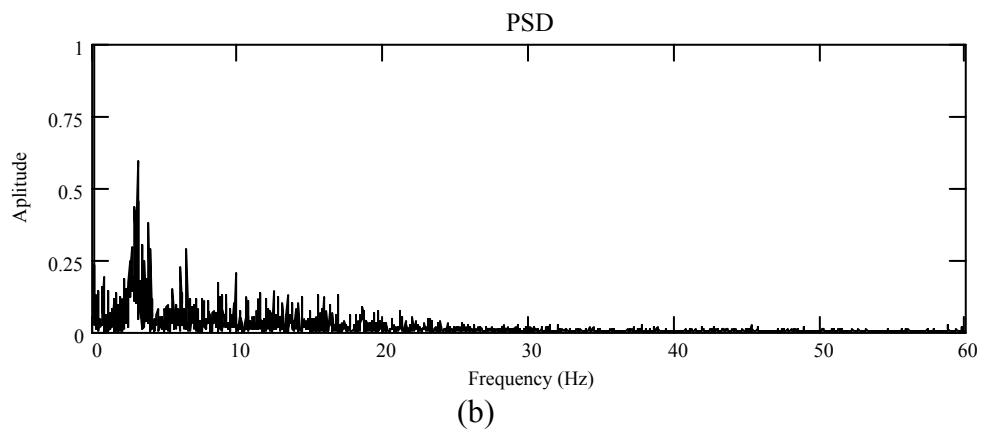
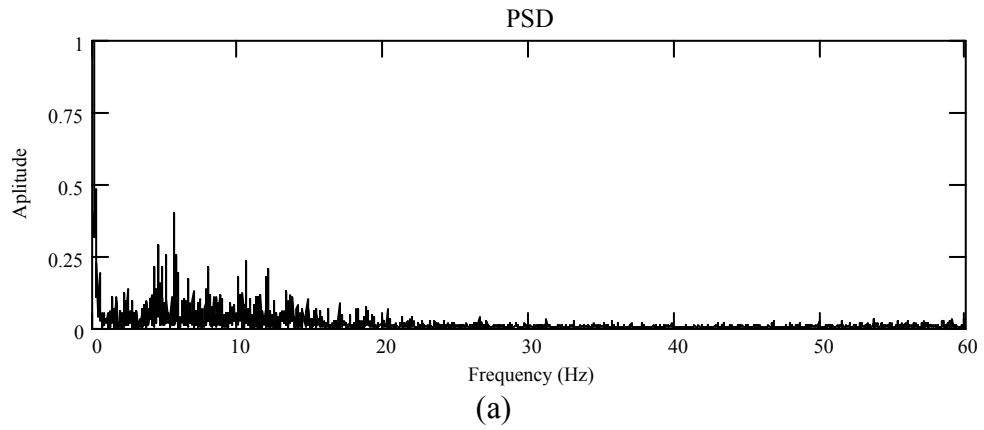
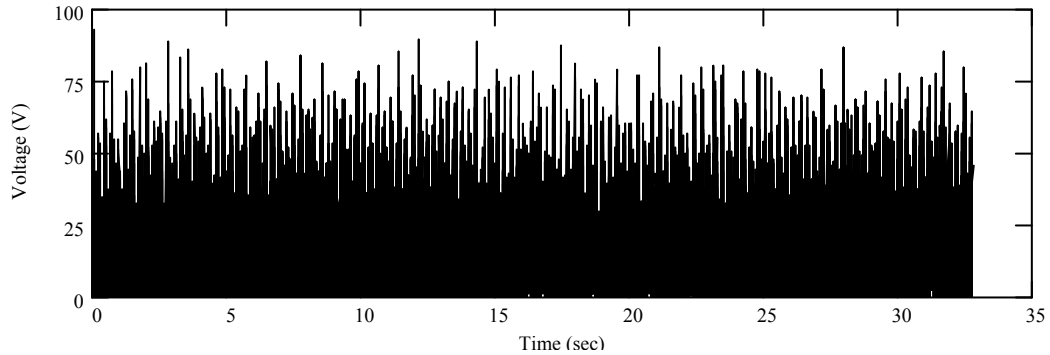


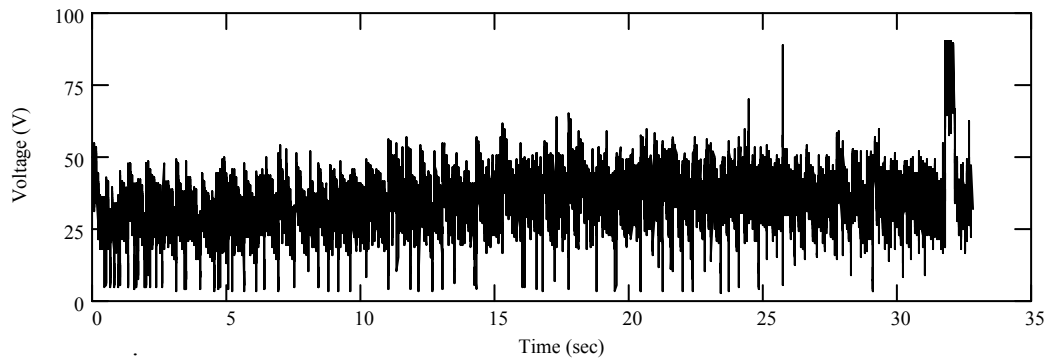
Figure A.17. Power spectral density of the voltage signals acquired during wet welding at 100 m with (a) E6013, (b) E7018, and (c) E7024 electrode type.

A.3.2 BOP welds on A572 Gr. 50 steel

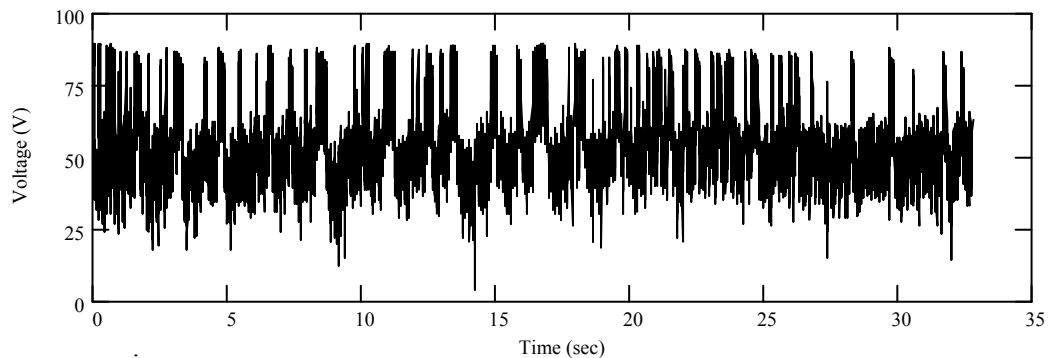
Figures A.18 and A.20 correspond to arc voltage signals in the time domain and its associated spectra are shown in Figure A.19 and A.21. The BOP wet welds were deposited with E6013, E7018, and E7024 electrode type on A572 Gr. 50 steel at 50 and 100m.



(a) Short-circuiting

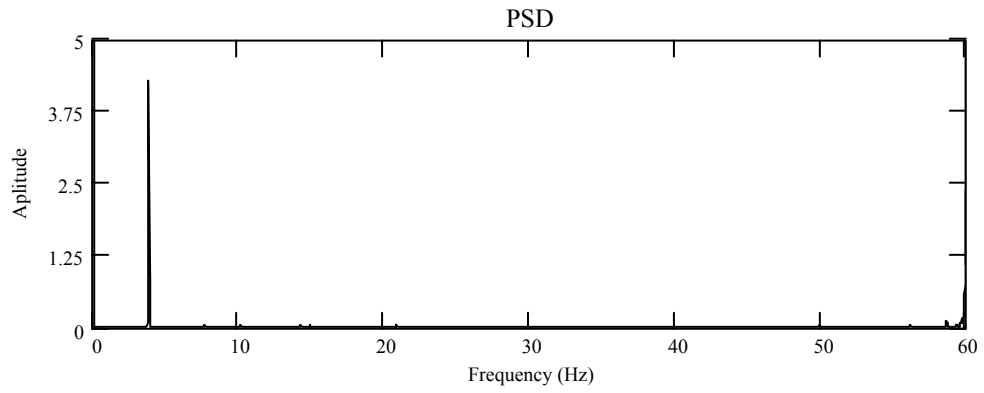


(b) Short-circuiting and globular

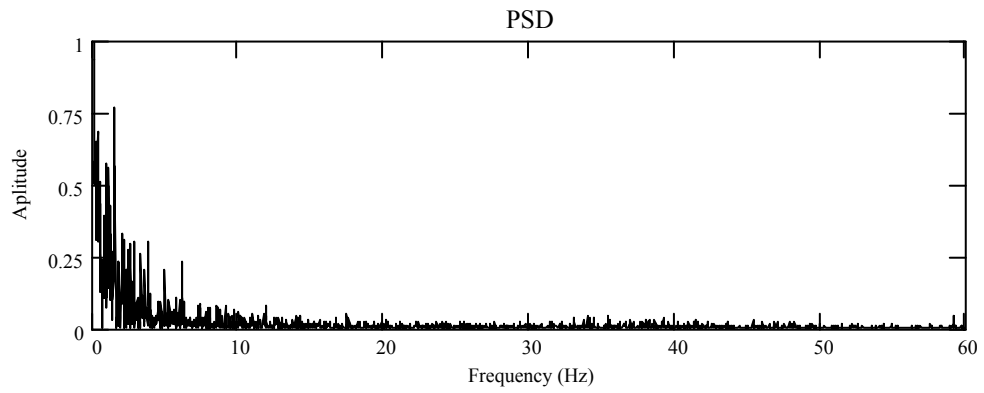


(c) Globular

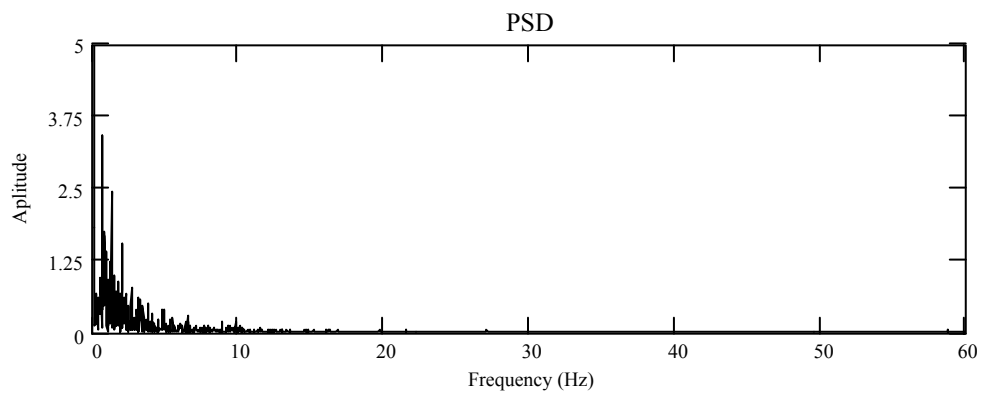
Figure A.18. Voltage signals recorded during wet welding with (a) E6013, (b) E7018, and (c) E7024 electrode type on A572 Gr. 50 steel at 50 m water depth.



(a)

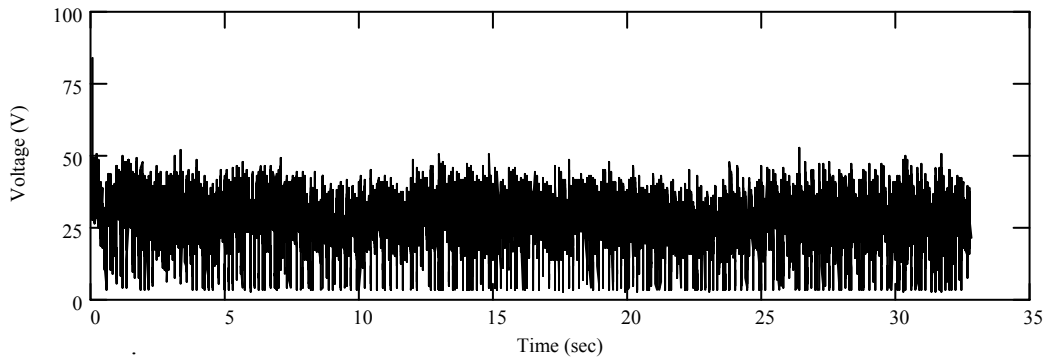


(b)

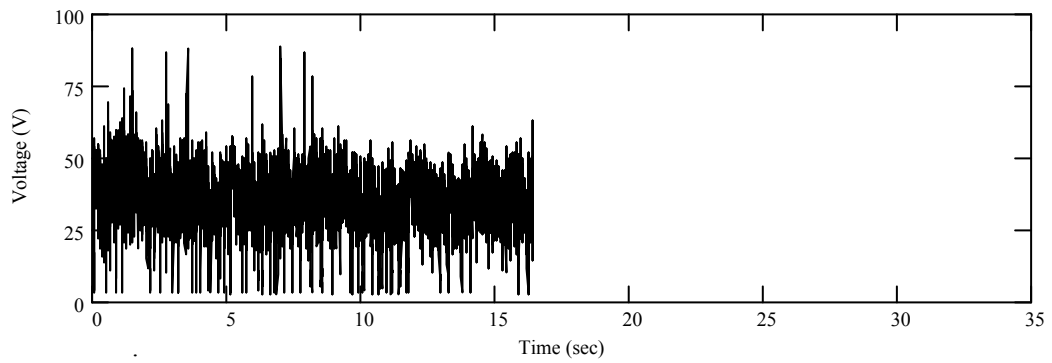


(c)

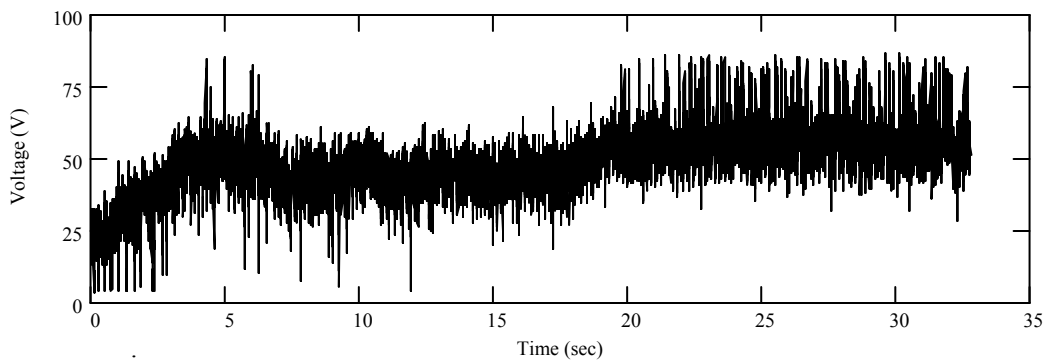
Figure A.19. Power spectral density of the voltage signals acquired during wet welding at 50 m with (a) E6013, (b) E7018, and (c) E7024 electrode type on A572 Gr. 50 steel.



(a) Short-circuiting

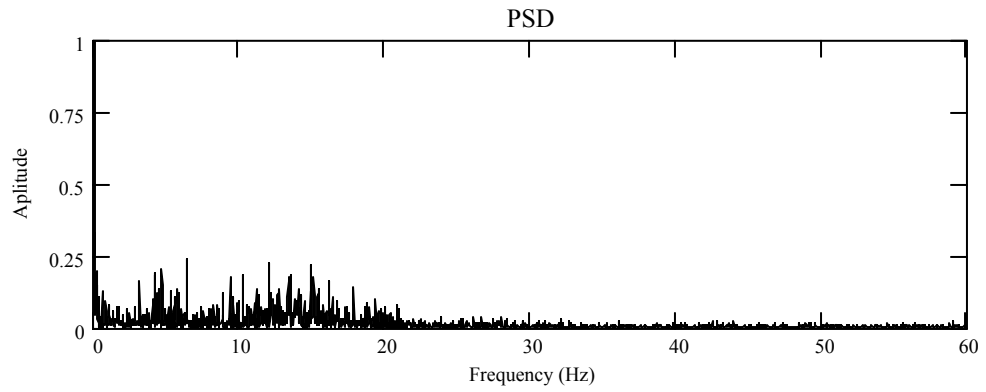


(b) Short-circuiting

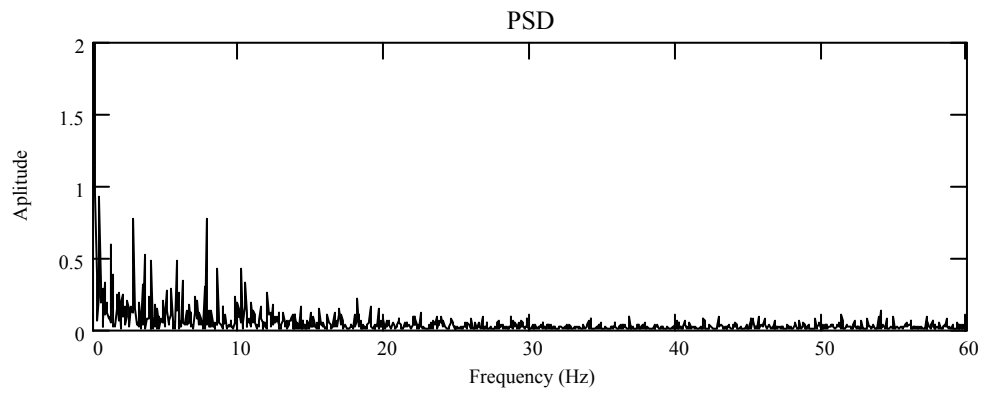


(c) Short-circuiting in the first 3 sec. then globular

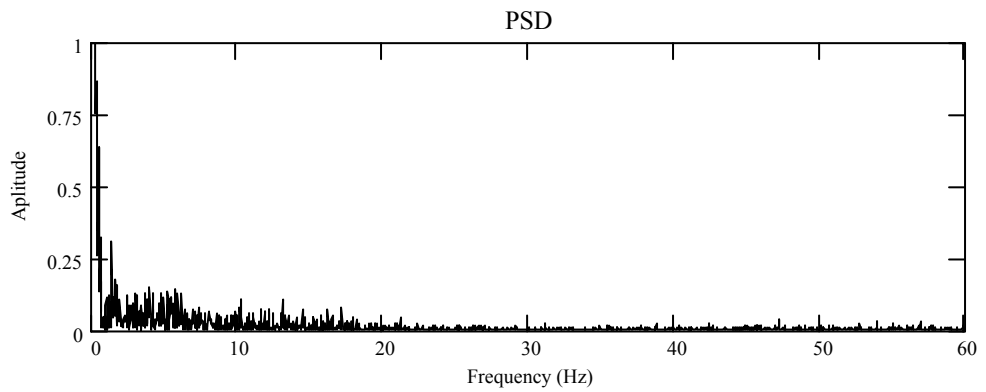
Figure A.20. Voltage signals recorded during wet welding with (a) E6013, (b) E7018, and (c) E7024 electrode type on A572 Gr. 50 steel at 100 m water depth.



(a)



(b)

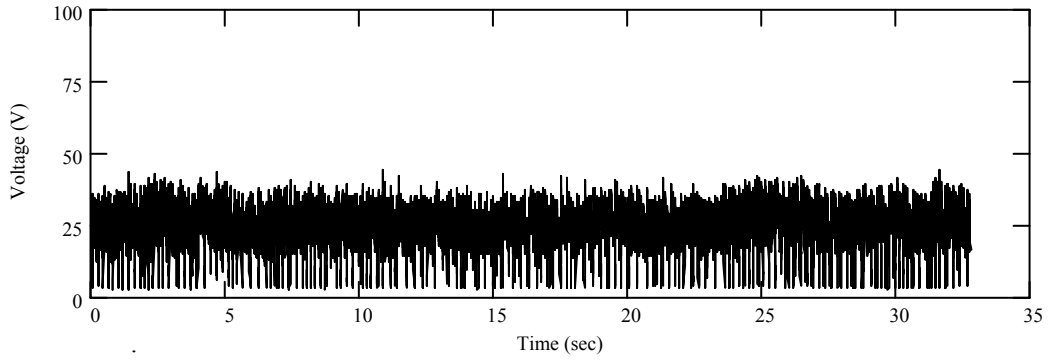


(c)

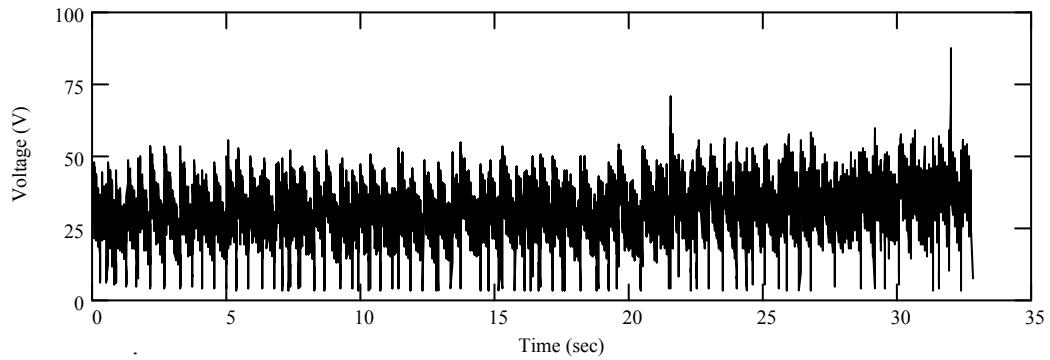
Figure A.21. Power spectral density of the voltage signals acquired during wet welding at 100 m with (a) E6013, (b) E7018, and (c) E7024 electrode type on A572 Gr. 50 steel.

A.3.3 BOP welds on API 5L Gr. B steel

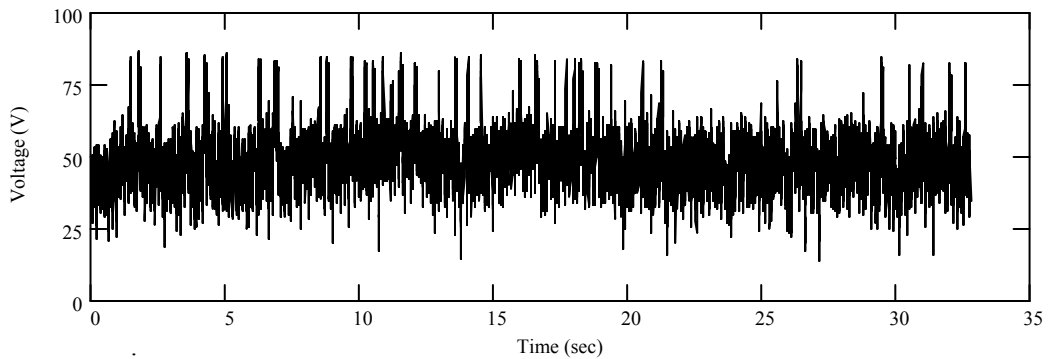
Figures A.22 and A.24 correspond to arc voltage signals in the time domain and its associated spectra are shown in Figure A.23 and A.25. The BOP wet welds were deposited with E6013, E7018, and E7024 electrode type on API 5L Gr. B steel at 50 and 100m.



(a) Short-circuiting

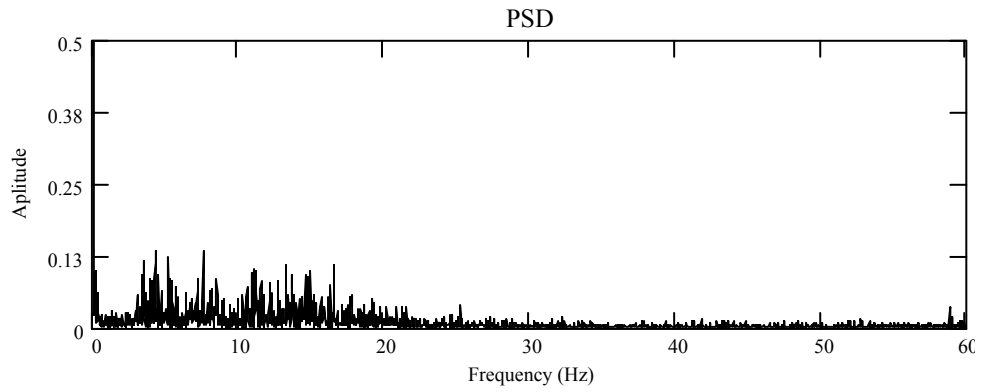


(b) Short-circuiting

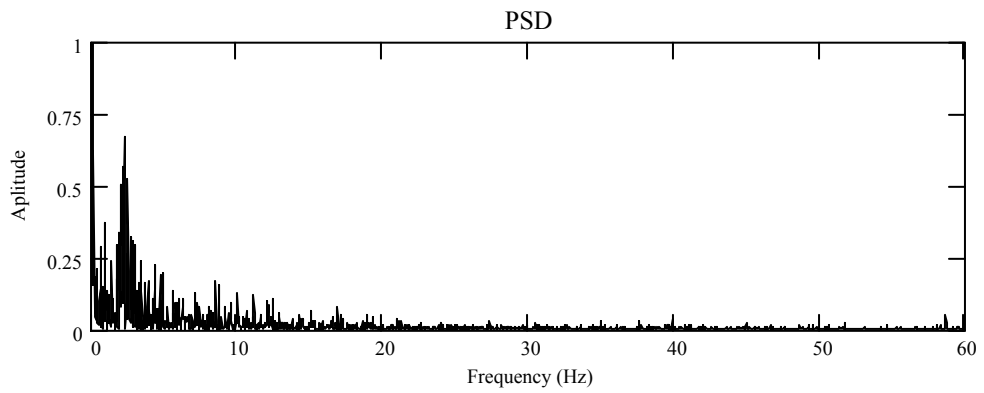


(c) Globular

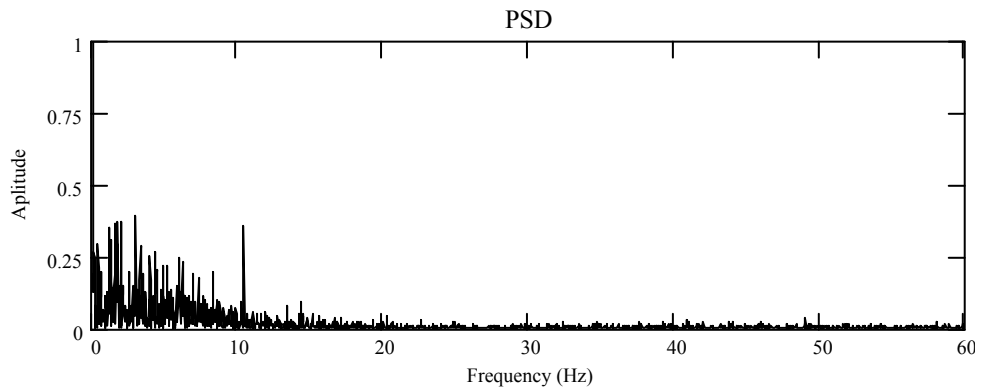
Figure A.22. Voltage signals recorded during wet welding with (a) E6013, (b) E7018, and (c) E7024 electrode type on API 5L Gr. B steel at 50 m water depth.



(a)

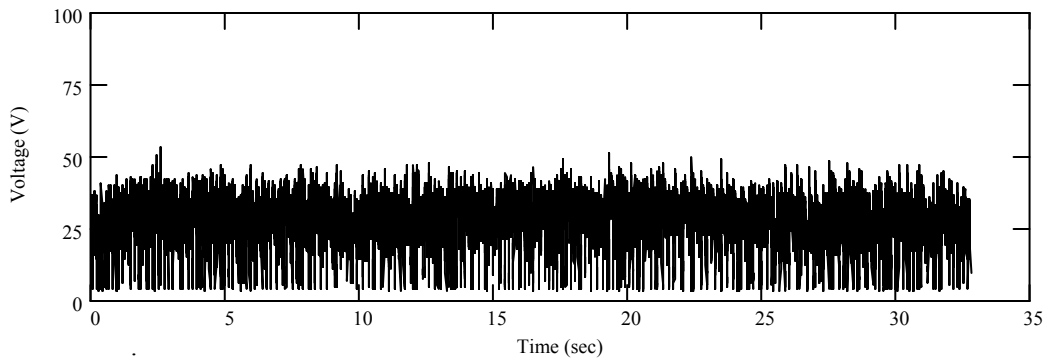


(b)

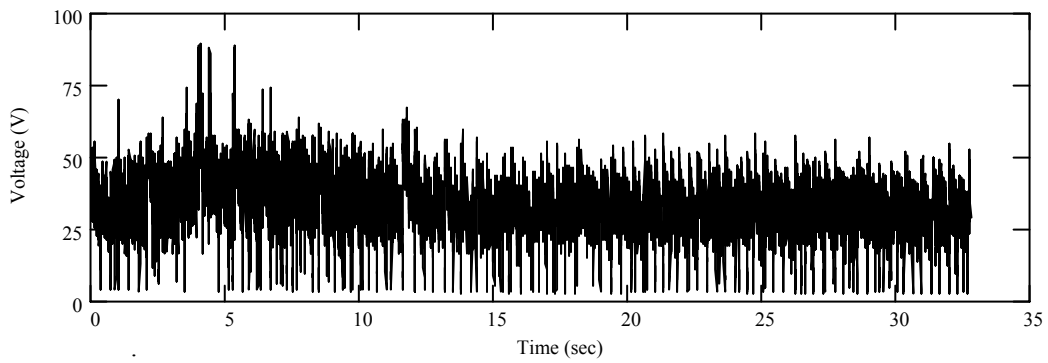


(c)

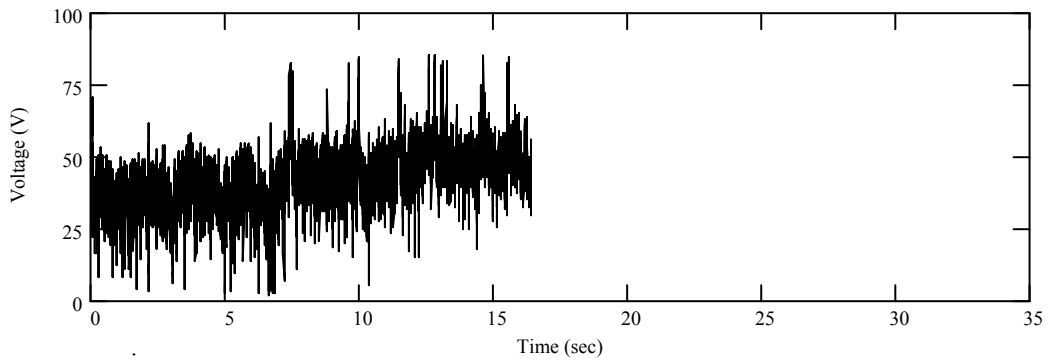
Figure A.23. Power spectral density of the voltage signals acquired during wet welding at 50 m with (a) E6013, (b) E7018, and (c) E7024 electrode type on API 5L Gr. B steel.



(a) Short-circuiting



(c) Short-circuiting



(d) Globular and short-circuiting

Figure A.24. Voltage signals recorded during wet welding with (a) E6013, (b) E7018, and (c) E7024 electrode type on API 5L Gr. B steel at 100 m water depth.

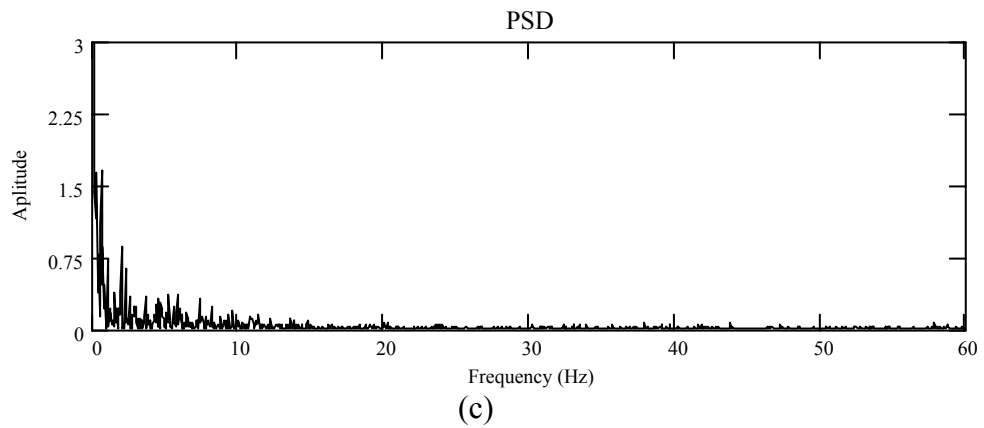
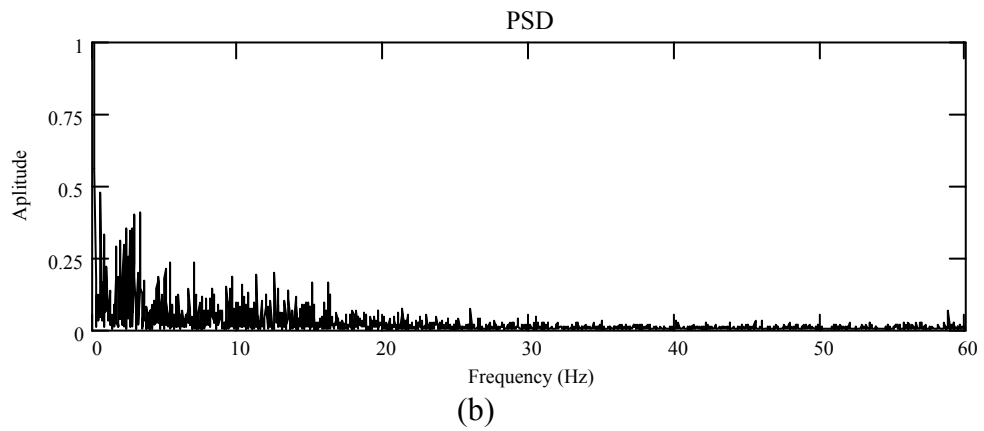
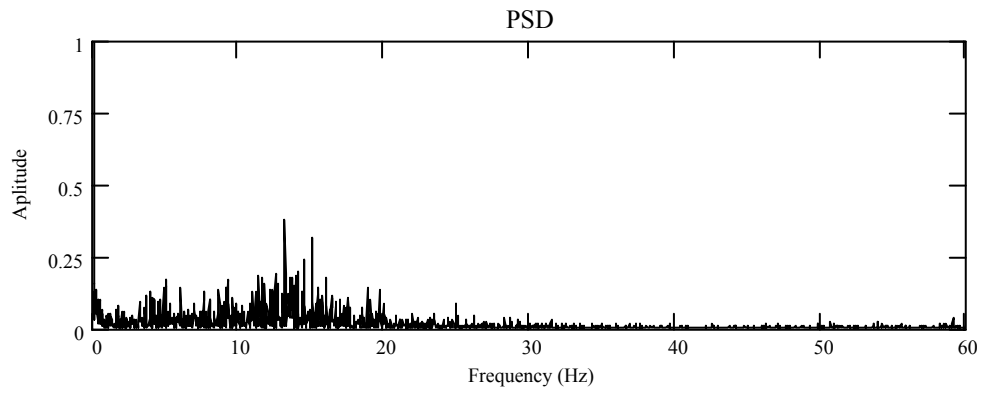


Figure A.25. Power spectral density of the voltage signals acquired during wet welding at 100 m with (a) E6013, (b) E7018, and (c) E7024 electrode type on API 5L Gr. B steel.

A.4 Arc current signals with direct current electrode positive (DCEP)

In order to assess the arc stability with each electrode type during wet welding, welding arc current signals were recorded. Figures A.26 to A.31 present the current signals acquired during welding with the three electrodes (E6013, E7018 and E7024) on the three steels at two water depths.

According to Madatov (1962) the arc stability can be defined as the maximum current divided by the minimum current with the following expression:

$$S = \frac{I_{\max}}{I_{\min}}$$

Where:

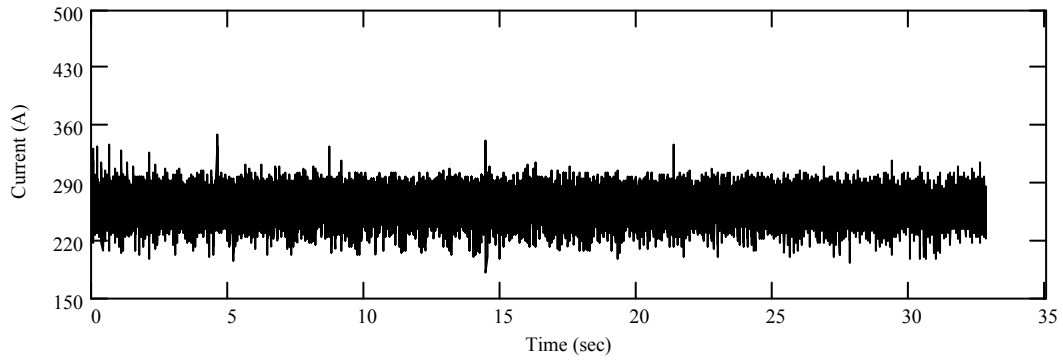
S is arc stability

I_{\max} is the maximum

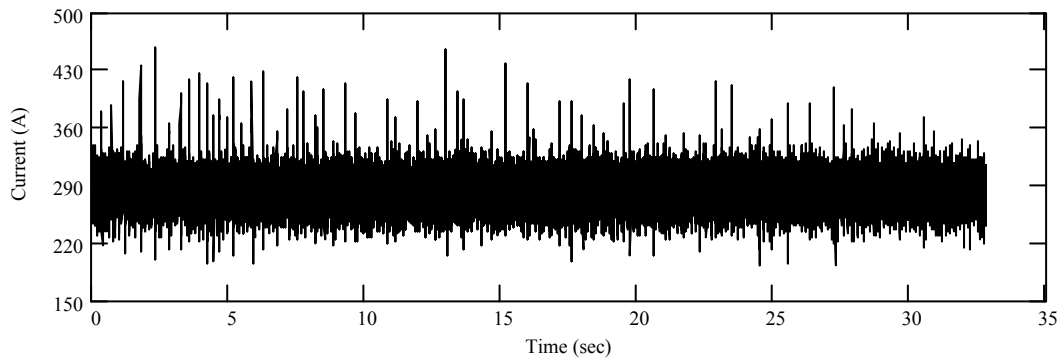
I_{\min} is the minimum current values

An arc is stable when the calculated S values are close to 1.0 and the arc is unstable when $S \gg 1.0$.

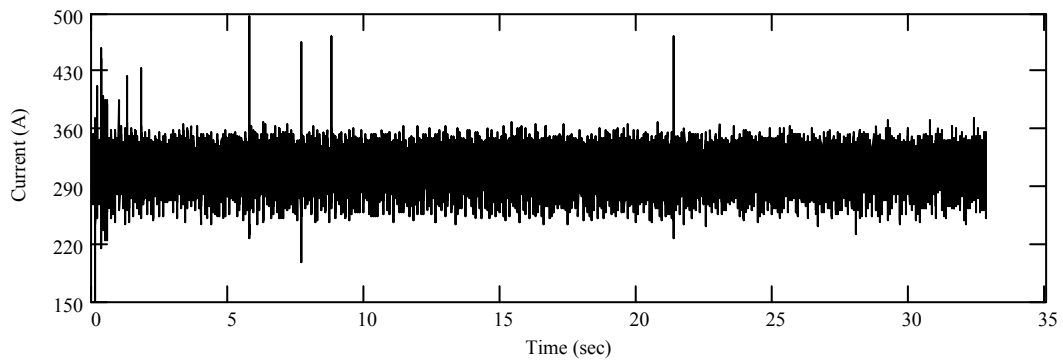
A.4.1 BOP welds on A36 steel



(a)

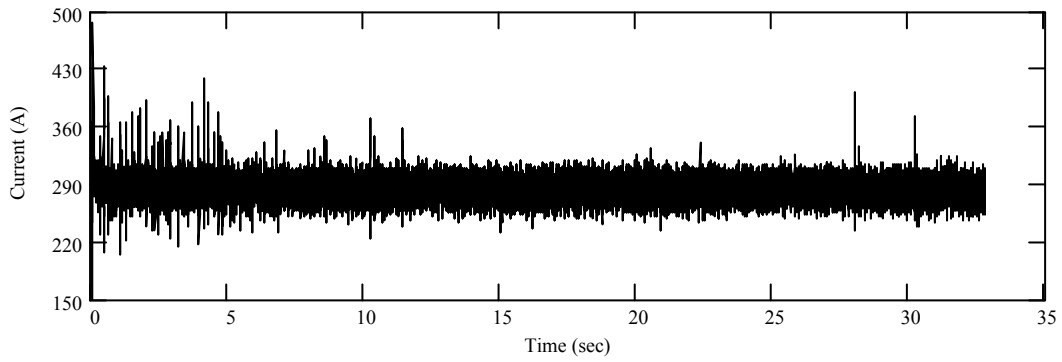


(b)

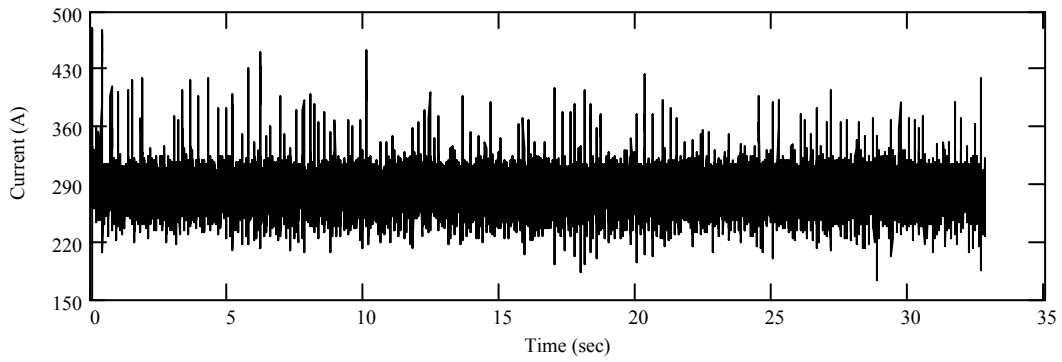


(c)

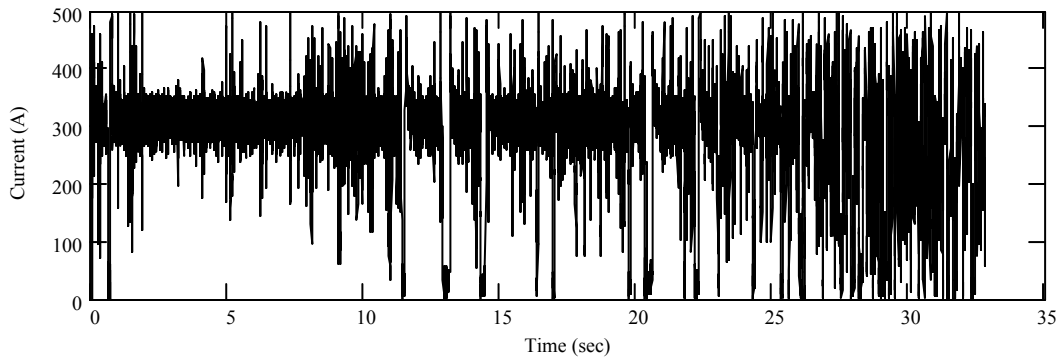
Figure A.26. Arc current signals from wet welds deposited with (a) E6013, (b) E7018, and (c) E7024 electrode type at 50 m.



(a)



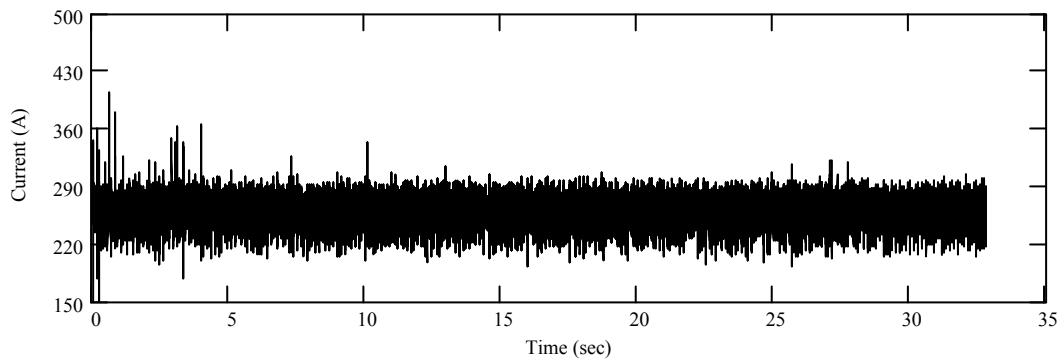
(b)



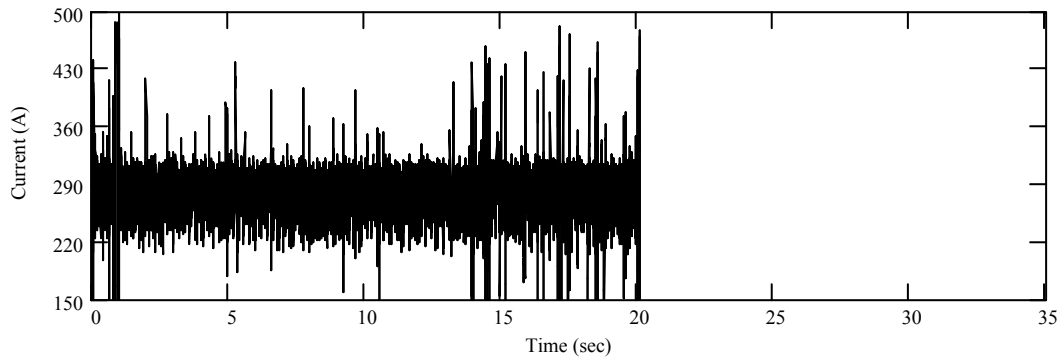
(c)

Figure A.27. Arc current signals from wet welds deposited with (a) E6013, (b) E7018, and (c) E7024 electrode type at 100 m.

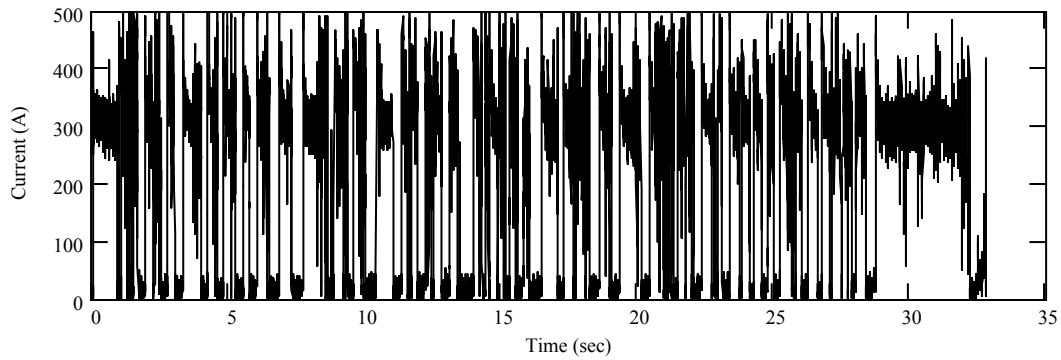
A.4.2 BOP welds on A572 Gr. 50 steel



(a)

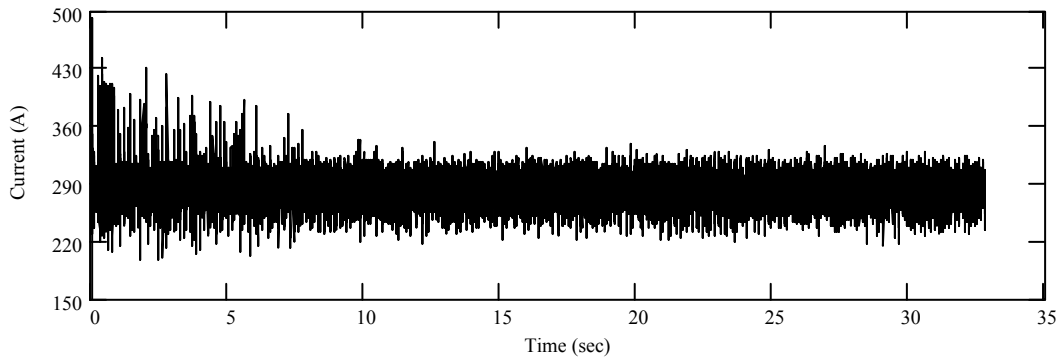


(b)

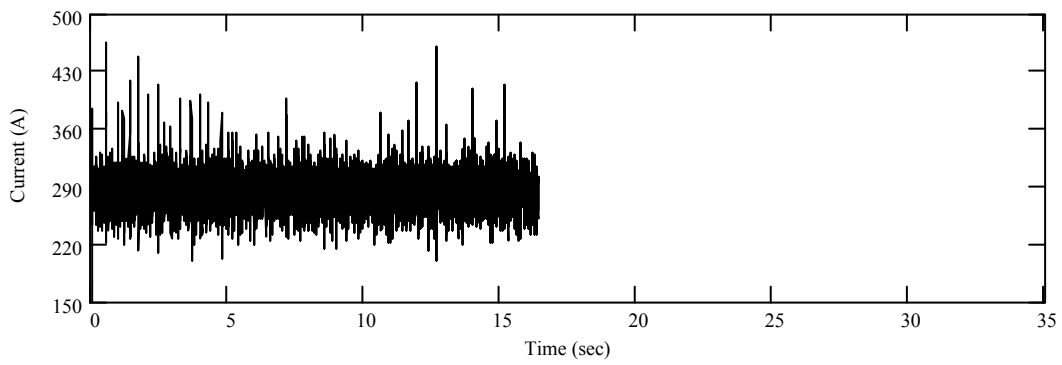


(c)

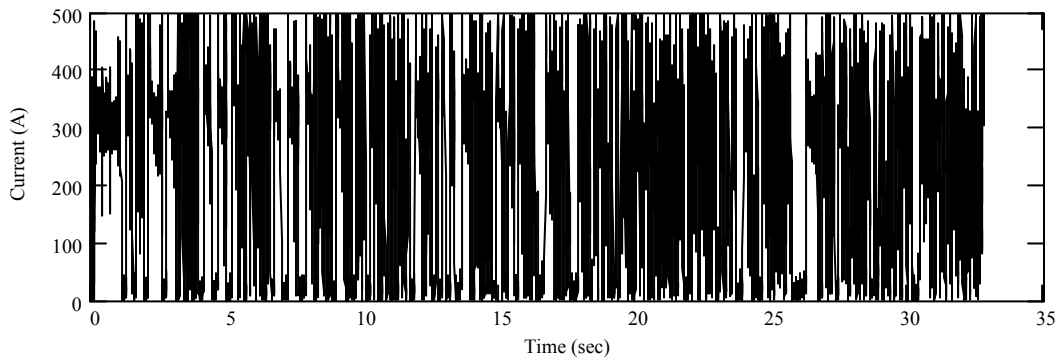
Figure A.28. Arc current signals from wet welds deposited with (a) E6013, (b) E7018, and (c) E7024 electrode type at 50 m.



(a)



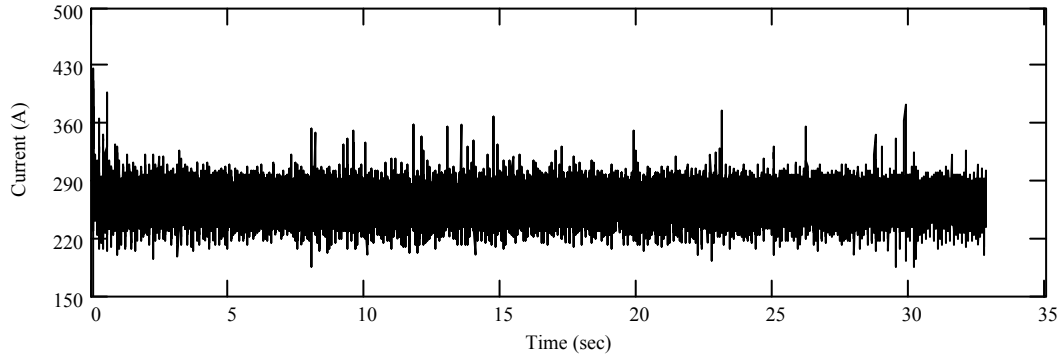
(b)



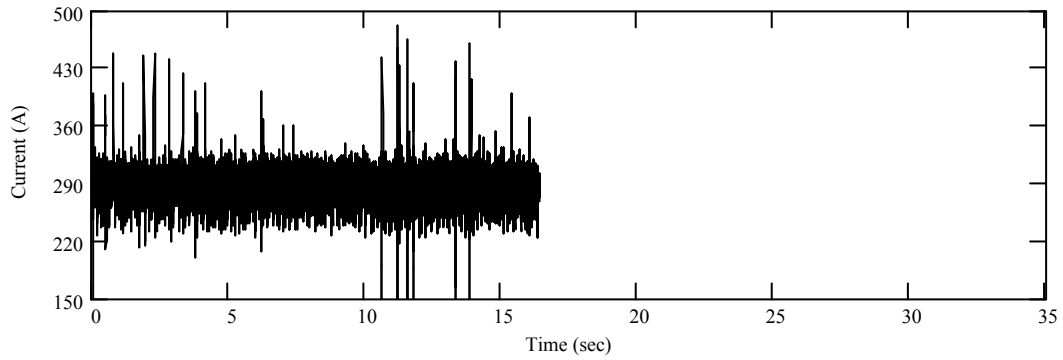
(c)

Figure A.29. Arc current signals from wet welds deposited with (a) E6013, (b) E7018, and (c) E7024 electrode type at 100 m.

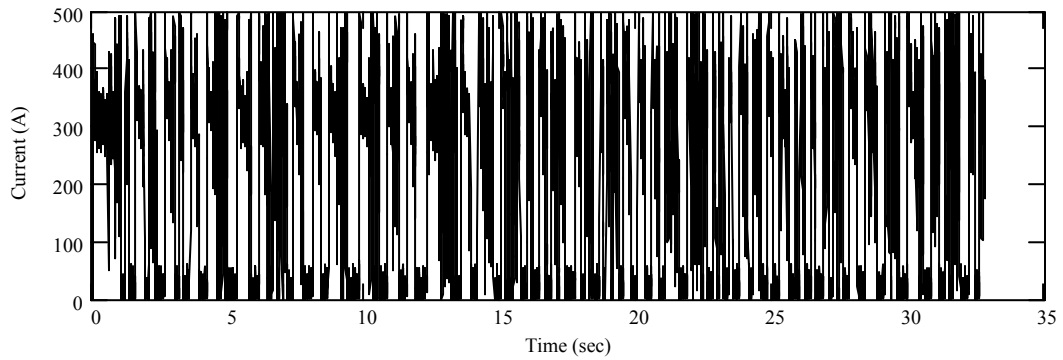
A.4.3 BOP welds on API 5L Gr. B steel



(a)

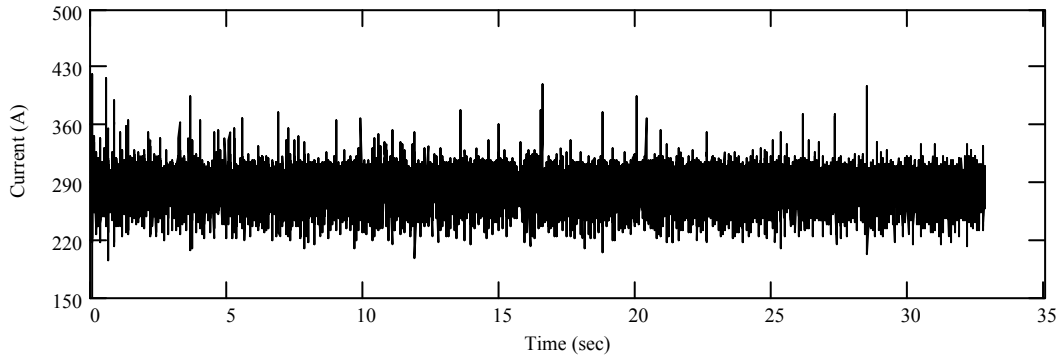


(b)

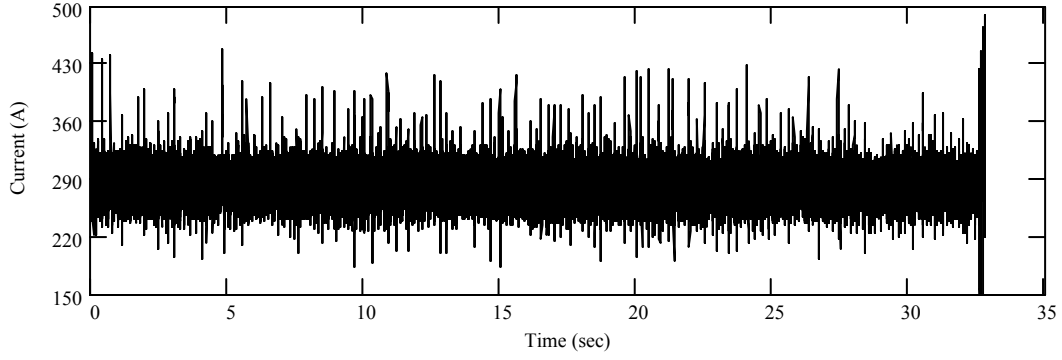


(c)

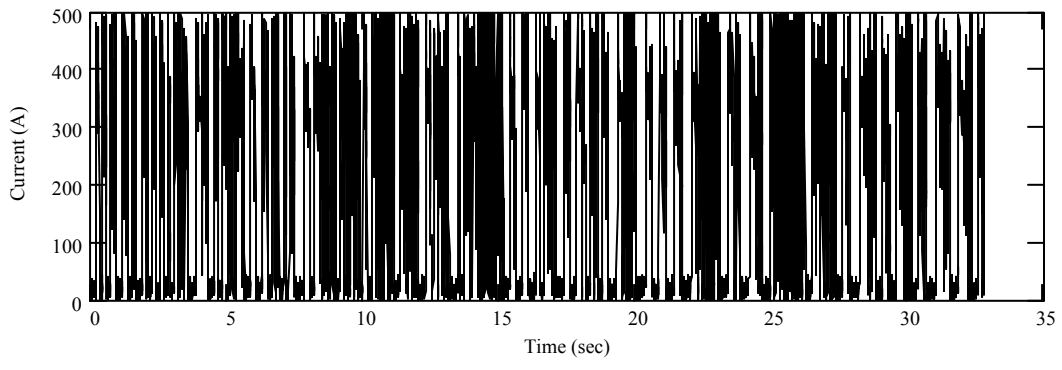
Figure A.30. Arc current signals from wet welds deposited with (a) E6013, (b) E7018, and (c) E7024 electrode type at 50 m.



(a)



(b)



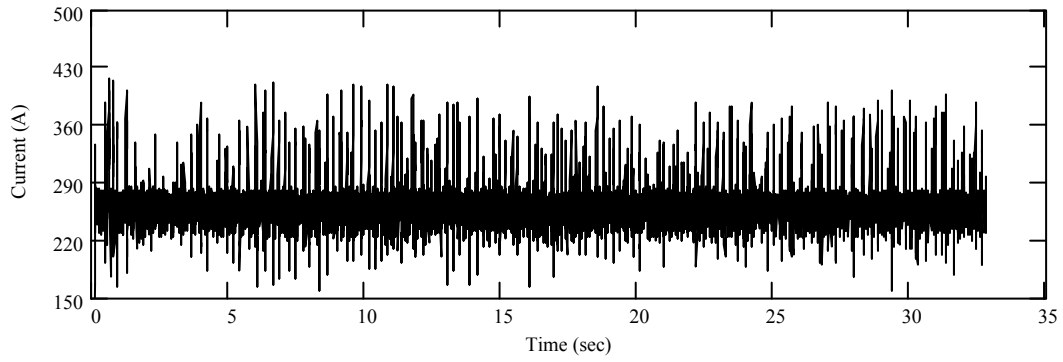
(c)

Figure A.31. Arc current signals from wet welds deposited with (a) E6013, (b) E7018, and (c) E7024 electrode type at 100 m.

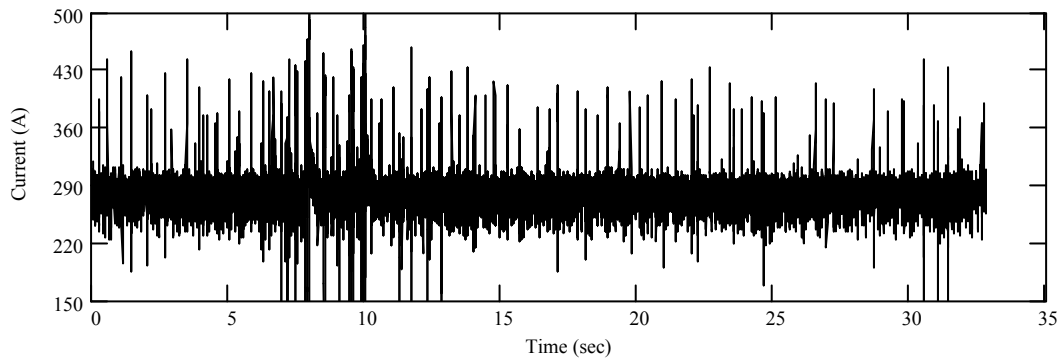
A.5 Arc current signals with direct current electrode negative (DCEN)

Figures A.32 to A.37 present the current signals acquired during welding with the three electrodes on the three steels at two water depths.

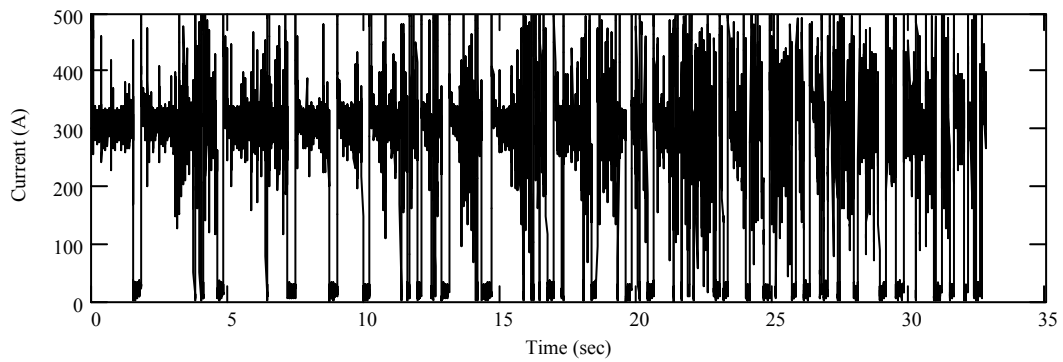
A.5.1 BOP welds on A36 steel



(a)

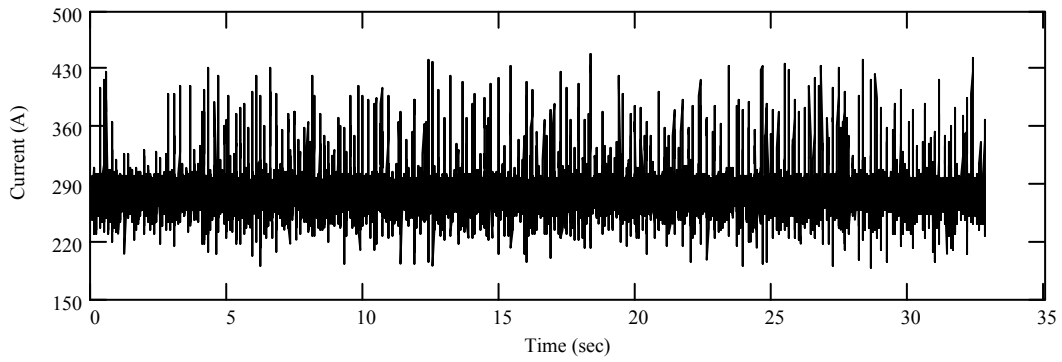


(b)

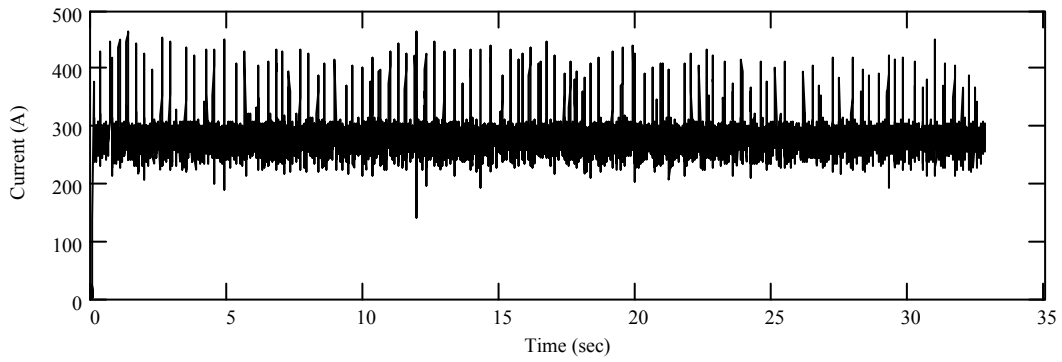


(c)

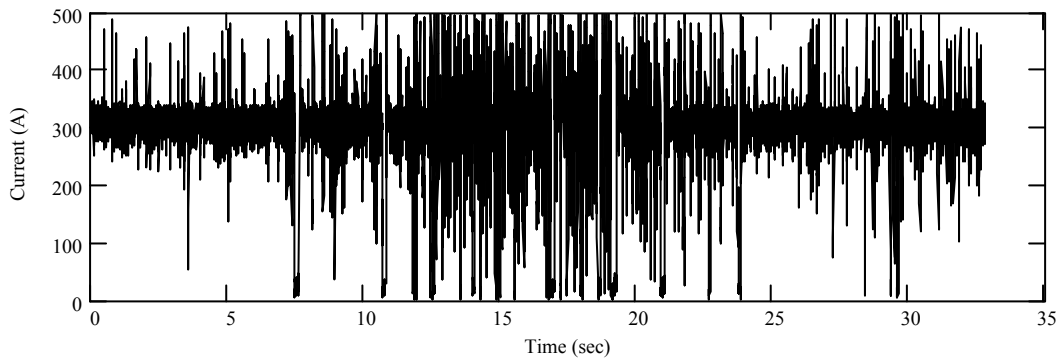
Figure A.32. Arc current signals from wet welds deposited with (a) E6013, (b) E7018, and (c) E7024 electrode type at 50 m.



(a)



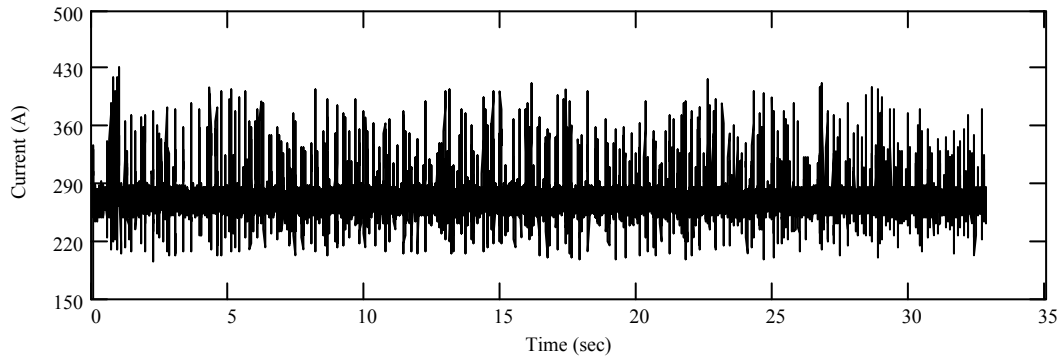
(b)



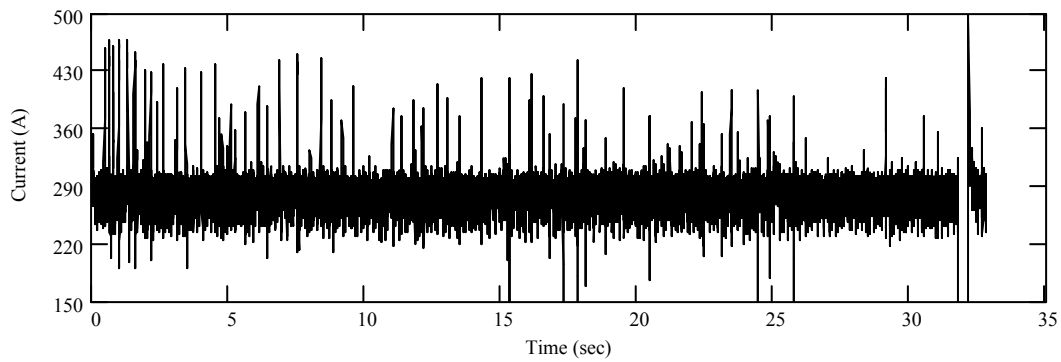
(c)

Figure A.33. Arc current signals from wet welds deposited with (a) E6013, (b) E7018, and (c) E7024 electrode type at 100 m.

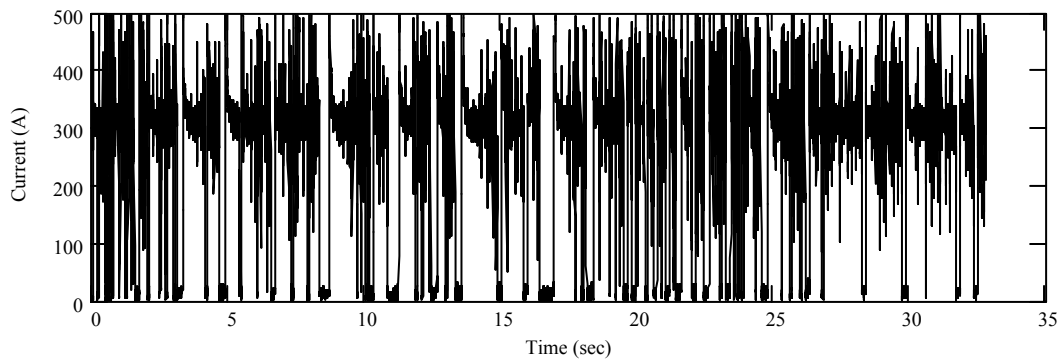
A5.2 BOP welds on A572 Gr. 50 steel



(a)

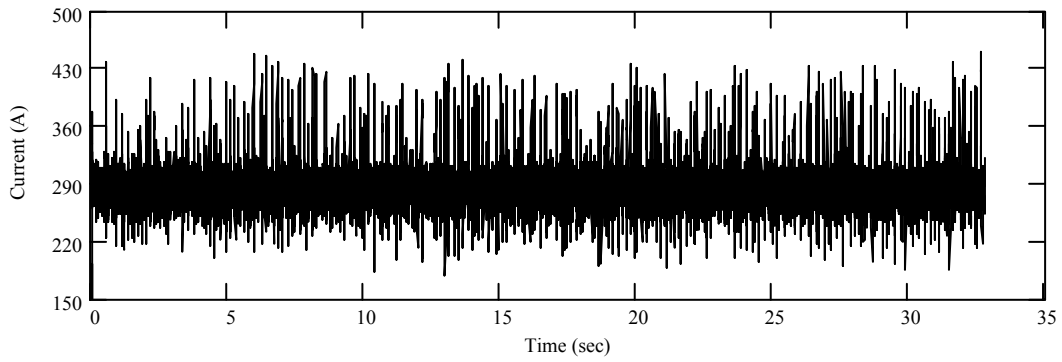


(b)

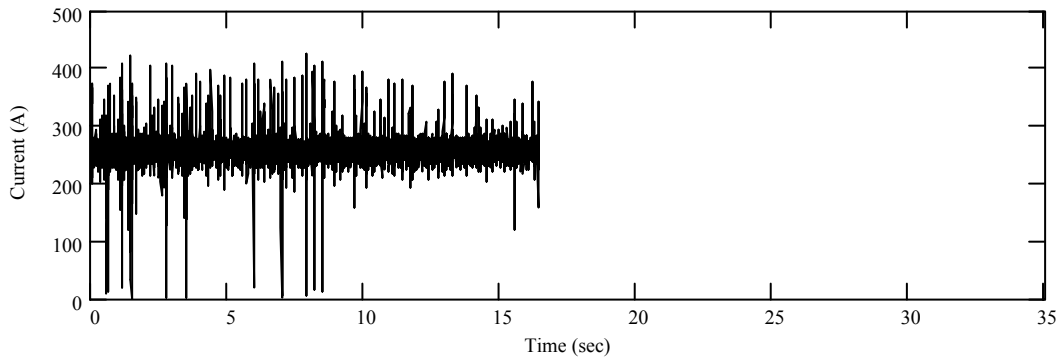


(c)

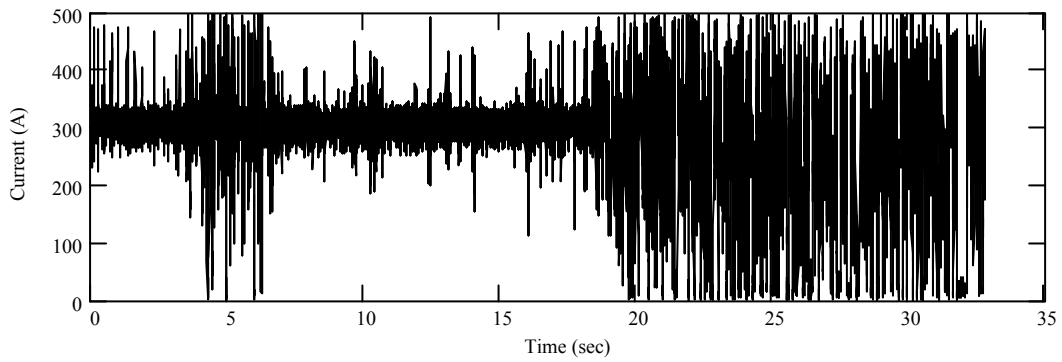
Figure A.34. Arc current signals from wet welds deposited with (a) E6013, (b) E7018, and (c) E7024 electrode type at 50 m.



(a)



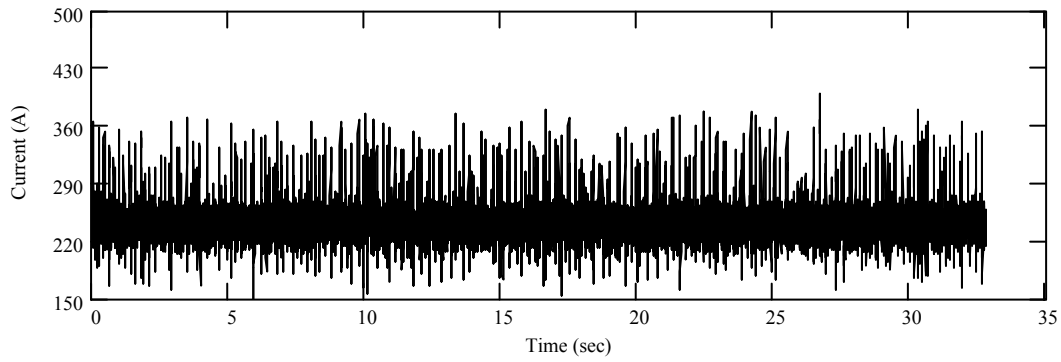
(b)



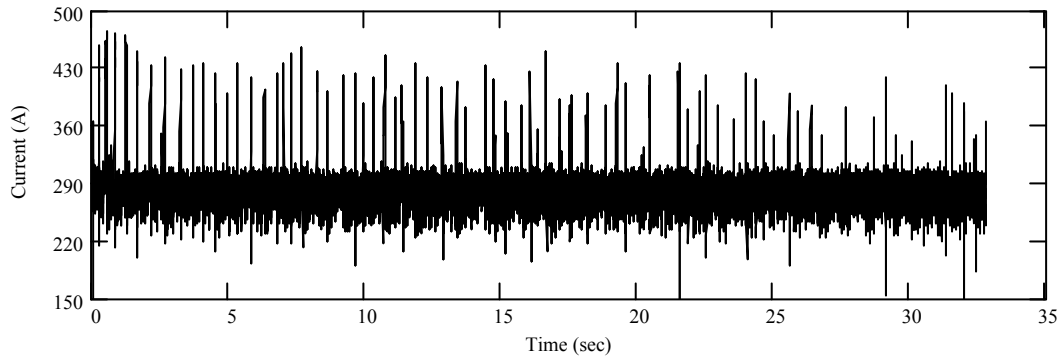
(c)

Figure A.35. Arc current signals from wet welds deposited with (a) E6013, (b) E7018, and (c) E7024 electrode type at 100 m.

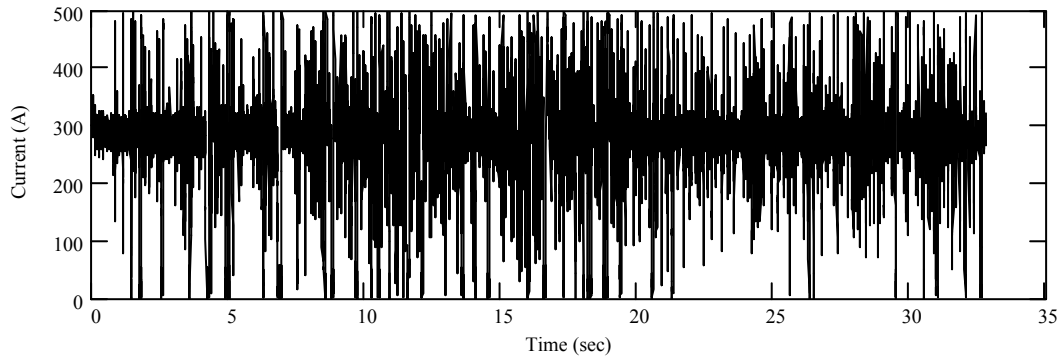
A.5.3 BOP welds on API 5L Gr. B



(a)

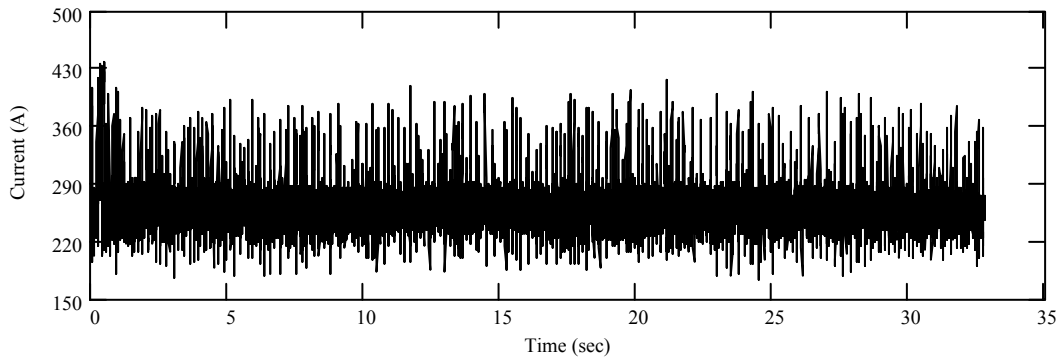


(b)

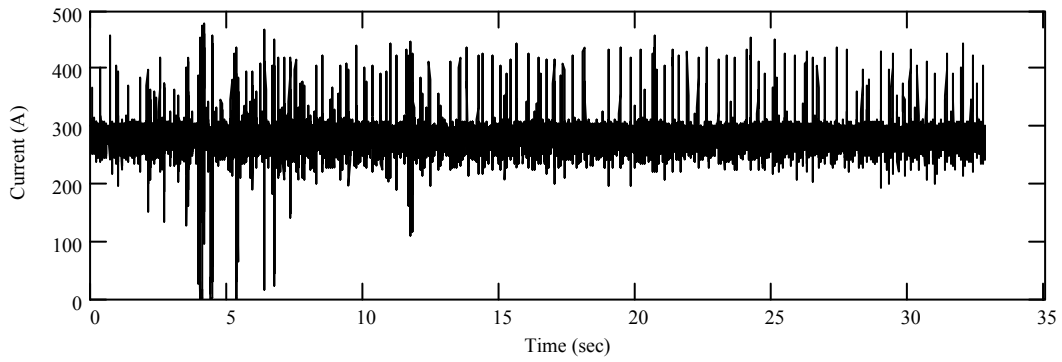


(c)

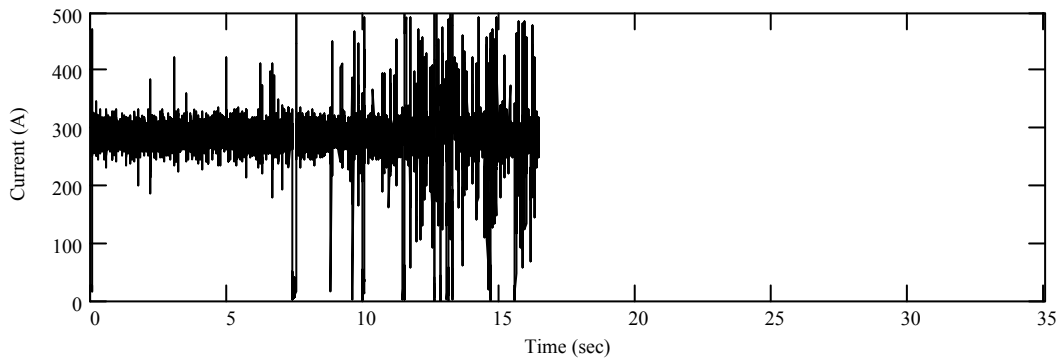
Figure A.36. Arc current signals from wet welds deposited with (a) E6013, (b) E7018, and (c) E7024 electrode type at 50 m.



(a)



(b)



(c)

Figure A.37. Arc current signals from wet welds deposited with (a) E6013, (b) E7018, and (c) E7024 electrode type at 100 m.

A.6 Summary of results

From the arc signals the average current, voltage, welding speed and heat input values were calculated, the values are given in Table 1. From table 1 one can see that voltage values in the range from 26 to 29 V were obtained with the E6013 electrode type using DCEP polarity, from 30 to 36 V were given by the E7018 and E6013 electrode, and the largest voltage values from 43 to 61 V corresponded to the E7024 electrode. This indicates that the arc length during wet welding with the E6013 electrode type was the smallest, medium for the E7018 electrode type, and the largest arc length for the E7024 electrode type. For the same electrode diameter, large arc lengths imply large arc volume that could contain larger amounts of hydrogen, oxygen, and other gases resulted from chemical reactions in the arc. Large amounts of gases in the arc could result in large amounts of porosity in the solidified wet weld metal.

Table A.2. Summary of welding parameter from the bead-on-plate wet welds deposited with three electrodes on three steel types and at two water depths.

BOP Weld	Polarity	Steel	Electrode	Water Depth, m	Selected Current, A	Avg. Current, A	Avg. Voltage, V	WS in/min	Heat Input kJ/in
11111	DCEP	A36	E6013	50	260	263.1	28.6	11.15	40.49
12112	DCEP	A36	E7018	50	280	284.1	31.4	11.49	46.57
13111	DCEP	A36	E7024	50	310	313	43.8	12.66	64.97
11211	DCEP	A36	E6013	100	280	284.9	30.6	12.12	43.16
12212	DCEP	A36	E7018	100	280	284.8	29.9	12.57	40.66
13211	DCEP	A36	E7024	100	310	280	50.8	10.91	78.20
21111	DCEP	A572-Gr.50	E6013	50	260	261.4	32.4	11.55	43.99
22113	DCEP	A572-Gr.50	E7018	50	280	278.1	36	11.62	51.69
23111	DCEP	A572-Gr.50	E7024	50	310	216.7	57.9	9.33	80.68
21211	DCEP	A572-Gr.50	E6013	100	280	285.2	28.4	12.09	40.18
22212	DCEP	A572-Gr.50	E7018	100	280	252.9	30.6	11.98	38.77
23211	DCEP	A572-Gr.50	E7024	100	310	203	59	8.95	80.27
31111	DCEP	API 5L Gr. B	E6013	50	260	264.7	25.9	10.54	39.04
32112	DCEP	API 5L Gr. B	E7018	50	280	286.3	34.4	11.74	50.33
33111	DCEP	API 5L Gr. B	E7024	50	310	195	60.2	8.69	81.02
31211	DCEP	API 5L Gr. B	E6013	100	280	283.8	27.3	12.09	38.44
32211	DCEP	API 5L Gr. B	E7018	100	280	283.8	30.5	12.12	42.86
33211	DCEP	API 5L Gr. B	E7024	100	310	186.1	60.3	9.14	73.65
11113	DCEN	A36	E6013	50	260	264.7	24.16	8.60	44.63
12114	DCEN	A36	E7018	50	280	282.1	33.2	9.80	57.32
13113	DCEN	A36	E7024	50	310	252.7	53.1	8.50	94.67
11213	DCEN	A36	E6013	100	280	285.1	27.8	10.56	45.04
12213	DCEN	A36	E7018	100	280	285.5	30	10.35	49.67
13213	DCEN	A36	E7024	100	310	293.9	45.9	11.01	73.53
21113	DCEN	A572-Gr.50	E6013	50	260	273.6	19.2	7.54	41.83
22114	DCEN	A572-Gr.50	E7018	50	280	282	33.4	9.12	61.98
23112	DCEN	A572-Gr.50	E7024	50	310	251.3	54.7	8.74	94.37
21213	DCEN	A572-Gr.50	E6013	100	280	289.3	25.9	9.09	49.43
22213	DCEN	A572-Gr.50	E7018	100	280	261.6	34.8	10.46	52.20
23213	DCEN	A572-Gr.50	E7024	100	310	271	49.3	8.43	95.06
31113	DCEN	API 5L Gr. B	E6013	50	260	246.2	22.9	8.03	42.12
32113	DCEN	API 5L Gr. B	E7018	50	280	285.3	30.1	10.02	51.44
33113	DCEN	API 5L Gr. B	E7024	50	310	265.8	49.4	9.52	82.76
31213	DCEN	API 5L Gr. B	E6013	100	280	265.3	25.7	9.14	44.75
32213	DCEN	API 5L Gr. B	E7018	100	280	285.8	32.3	16.68	33.21
33213	DCEN	API 5L Gr. B	E7024	100	310	278.4	42.4	9.97	71.05

In the case of DCEN polarity the smallest voltage were in the range values from 19 to 28 V for the E6013, voltage values from 30 to 35 V were for the E7018, and the largest values from 42 to 55 V were for the E7024 electrode type.

It is important to mention that the E7024 electrode type had the thickest flux covering. Iron powder is added to the flux covering to increase the deposition rate. Thereafter, this electrode type requires higher current values (310 A). Also, thicker flux covering implies larger arc voltage values or larger arc length.

Heat input values vary from 38 to 52 kJ/in for the E6013 and E7018 electrode type and from 64 to 81 kJ/in for the E7024 when using DCEP. With DCEN polarity heat input values were in the range from 40 to 49 kJ/in for the E6013, from 49 to 62 kJ/in for the E7018, and from 71 to 95 kJ/in for the E7024 electrode type.

Based on the arc signal analysis the dominant metal transfer modes during wet welding with the three electrodes on the three steel plates at 50 and 100 m water depth are given in Table 2.

Table A.3. Metal transfer modes observed in wet welds deposited with three electrode types on three steels at two water depths.

Steel plate	Electrode	At 50 m		At 100 m	
		Metal transfer modes	Metal transfer frequency (Hz)	Metal transfer modes	Metal transfer frequency (Hz)
A36	E6013	G	0-10	G and SC	0-21
	E7018	SC	0-5	SC	0-15
	E7024	G	0-9	G	0-5
A572 Gr. 50	E6013	G	0-7	G and SC	0-20
	E7018	SC and G	0-6	SC	0-10
	E7024	G	0-3	G	0-5 & 11-15
API 5L Gr. B	E6013	SC and G	0-20	SC and G	0-21
	E7018	SC and G	0-3	SC	0-5
	E7024	G	0-3	G	2.5

Note: G stands for globular and SC stands for short-circuiting

Signals of the arc current showed very large fluctuation for the E7024 electrode type, which implies large S values or unstable arc. However this is not in agreement with the observed arc behavior. Taking into consideration the ability to start the arc and arc extinction, the E7024 electrode presented the best arc stability in all cases. On the other hand, from the arc current signals the E7018 electrode type presented better arc stability than the E7024 electrode type. Based on the ability to start the arc and arc extinction this electrode presented unstable arcs. The E6013 electrode type presented good arc stability with DCEP.